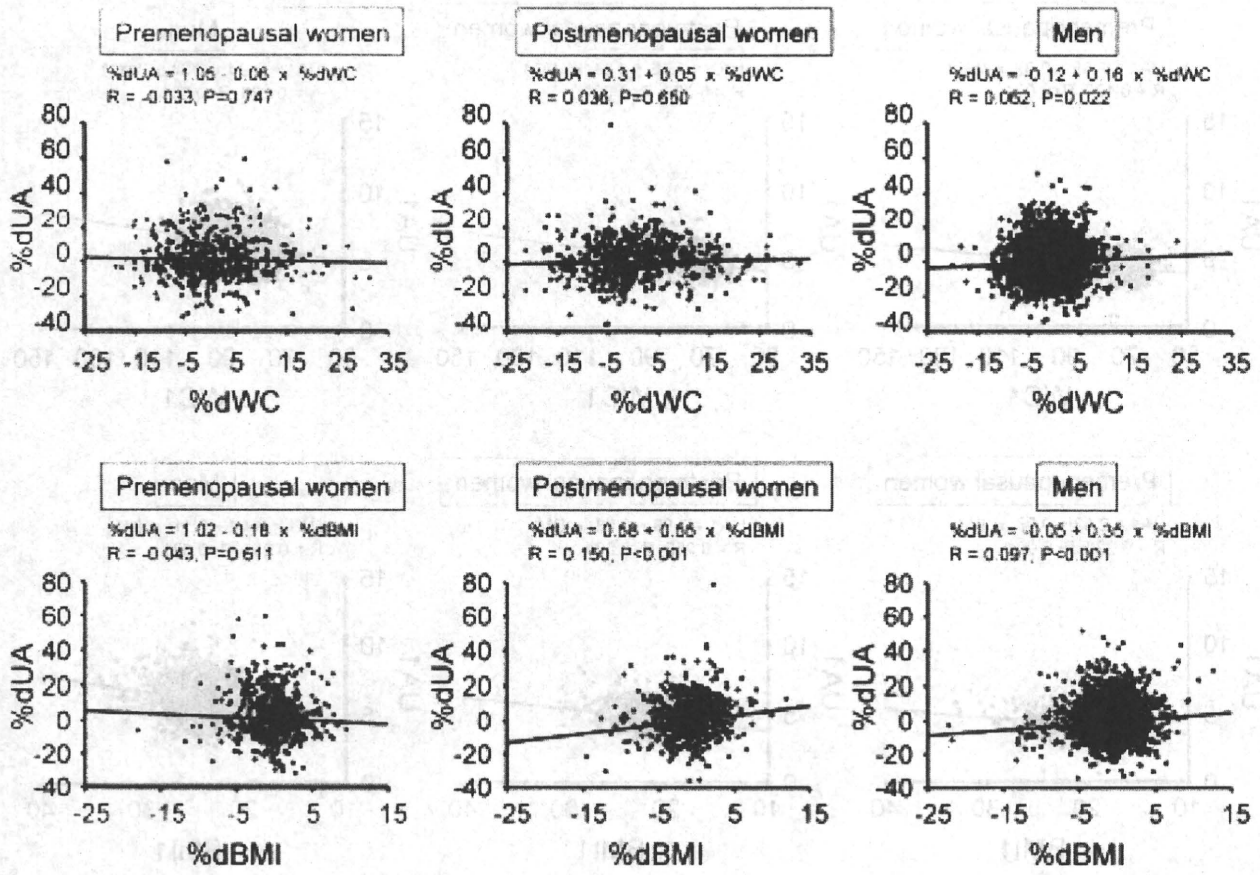

Figure 2. Scatterplot and linear regression between percentage change in waist circumference (%dWC) and percentage change in uric acid (%dUA), and those between percentage change in BMI (%dBMI) and %dUA in premenopausal and postmenopausal women and in men. Serum uric acid values were not adjusted for age or other possible confounders.

general/abdominal obesity, as no program to reduce weight was conducted by our institute. Second, we did not take into account participants' level of alcohol consumption or number of cigarettes smoked; both may affect serum UA levels[29,30]. Third, blood samples were taken from individuals in fasting condition, which may have affected their serum creatinine levels, and thus eGFR.

In summary, during a 1-year period, percentage changes in BMI (%dBMI) were associated positively with percentage changes in serum UA levels (%dUA) in postmenopausal women and men, but not in premenopausal women. This relationship was, at least in part, independent of changes in blood pressure and renal function. Weight loss may represent an effective strategy to decrease serum UA levels without use of antihyperuricemic medications, especially in postmenopausal women and men.

REFERENCES

1. Modan M, Halkin H, Karasik A, Lusky A. Elevated serum uric acid — a facet of hyperinsulinaemia. Diabetologia 1987;30:713-8.
2. Ishizaka N, Ishizaka Y, Toda E, Nagai R, Yamakado M. Association between serum uric acid, metabolic syndrome, and carotid atherosclerosis in Japanese individuals. Arterioscler Thromb Vasc Biol 2005;25:1038-44.
3. Ford ES, Li C, Cook S, Choi HK. Serum concentrations of uric acid and the metabolic syndrome among US children and adolescents. Circulation 2007;115:2526-32.
4. Gillum RF. The association of the ratio of waist to hip girth with blood pressure, serum cholesterol and serum uric acid in children and youths aged 6-17 years. J Chronic Dis 1987;40:413-20.
5. Kono S, Shinchi K, Imanishi K, Honjo S, Todoroki I. Behavioural and biological correlates of serum uric acid: a study of self-defence officials in Japan. Int J Epidemiol 1994;23:517-22.
6. Yamashita S, Matsuzawa Y, Tokunaga K, Fujioka S, Tarui S. Studies on the impaired metabolism of uric acid in obese subjects: marked reduction of renal urate excretion and its improvement by a low-calorie diet. Int J Obes 1986;10:255-64.
7. Rathmann W, Haastert B, Icks A, Fiani G, Roseman JM. Ten-year change in serum uric acid and its relation to changes in other metabolic risk factors in young black and white adults: the CARDIA study. Eur J Epidemiol 2007;22:439-45.
8. Masuo K, Kawaguchi H, Mikami H, Ogihara T, Tuck ML. Serum uric acid and plasma norepinephrine concentrations predict subsequent weight gain and blood pressure elevation. Hypertension 2003;42:474-80.
9. Choe JY, Park SH, Kim JY, Shin IH, Kim SK. Change in serum uric acid between baseline and 1-year follow-up and its associated factors in male subjects. Clin Rheumatol 2008;27:483-9.

Table 2. Stepwise multiple regression analysis using %dUA as the dependent variable.

	ß	(95% CI)	Standardized ß	p
Premenopausal women				
Model 1				
UA1	–4.21	(–5.42, –3.00)	–0.28	< 0.001
Model 2				
UA1	–4.21	(–5.42, –3.00)	–0.28	< 0.001
Model 3				
UA1	–4.21	(–5.42, –3.00)	–0.28	< 0.001
Model 4				
%deGFR	–0.43	(–0.53, –0.33)	–0.34	< 0.001
UA1	–3.70	(–4.84, –2.56)	–0.25	< 0.001
Model 5				
%deGFR	–0.43	(–0.53, –0.33)	–0.34	< 0.001
UA1	–3.70	(–4.84, –2.56)	–0.25	< 0.001
Postmenopausal women				
Model 1				
UA1	–3.09	(–4.05, –2.13)	–0.24	< 0.001
Model 2				
UA1	–3.04	(–4.00, –2.09)	–0.24	< 0.001
%dBMI	0.53	(0.26, 0.81)	0.14	< 0.001
Model 3				
UA1	–3.04	(–4.00, –2.09)	–0.24	< 0.001
%dBMI	0.53	(0.26, 0.81)	0.14	< 0.001
Model 4				
%deGFR	–0.33	(–0.41, –0.25)	–0.30	< 0.001
UA1	–2.83	(–3.73, –1.92)	–0.22	< 0.001
%dBMI	0.55	(0.29, 0.81)	0.15	< 0.001
Model 5				
%deGFR	–0.33	(–0.41, –0.25)	–0.30	< 0.001
UA1	–2.83	(–3.73, –1.92)	–0.22	< 0.001
%dBMI	0.55	(0.29, 0.81)	0.15	< 0.001
Men				
Model 1				
UA1	–2.51	(–2.90, –2.12)	–0.27	< 0.001
%dWC	0.14	(0.04, 0.25)	0.06	0.008
Model 2				
UA1	–2.49	(–2.88, –2.10)	–0.27	< 0.001
%dBMI	0.32	(0.17, 0.48)	0.09	< 0.001
Model 3				
UA1	–2.51	(–2.89, –2.12)	–0.27	< 0.001
%dBMI	0.38	(0.22, 0.54)	0.10	< 0.001
%dBPs	–0.06	(–0.10, –0.02)	–0.06	0.006
Model 4				
%deGFR	–0.36	(–0.40, –0.31)	–0.32	< 0.001
UA1	–2.29	(–2.66, –1.92)	–0.25	< 0.001
%dBMI	0.35	(0.21, 0.50)	0.10	< 0.001
Model 5				
%deGFR	–0.36	(–0.40, –0.31)	–0.32	< 0.001
UA1	–2.29	(–2.66, –1.92)	–0.25	< 0.001
%dBMI	0.35	(0.21, 0.50)	0.10	< 0.001

Model 1. Independent variables include age, UA1, WC1, and %dWC. Model 2. Independent variables include Model 1 + BMI1 and %dBMI. Model 3. Independent variables include Model 2 + %dBPs. Model 4. Independent variables include Model 2 + %deGFR. Model 5. Independent variables include Model 2 + %dBPs and %deGFR. UA: uric acid; BMI: body mass index; BPs: systolic blood pressure; eGFR: estimated glomerular filtration rate.

10. Kokubo Y, Okamura T, Yoshimasa Y, et al. Impact of metabolic syndrome components on the incidence of cardiovascular disease in a general urban Japanese population: the suita study. Hypertens Res. 2008;31:2027-2035.
11. Matsuo S, Imai E, Horio M, et al. Revised equations for estimated GFR from serum creatinine in Japan. Am J Kidney Dis 2009;53:982-92.
12. Imai E, Horio M, Nitta K, Yamagata K, Iseki K, Hara S, et al. Estimation of glomerular filtration rate by the MDRD study equation modified for Japanese patients with chronic kidney disease. Clin Exp Nephrol 2007;11:41-50.
13. Ishizaka N, Ishizaka Y, Toda E, Koike K, Seki G, Nagai R, et al. Association between chronic kidney disease and carotid intima-media thickening in individuals with hypertension and impaired glucose metabolism. Hypertens Res 2007;30:1035-41.
14. Ishizaka N, Ishizaka Y, Toda E, Koike K, Seki G, Nagai R, et al. Association between obesity and chronic kidney disease in Japanese: differences in gender and hypertensive status? Hypertens Res 2007;30:1059-64.
15. Ishizaka N, Ishizaka Y, Toda E, Shimomura H, Koike K, Seki G, et al. Association between cigarette smoking and chronic kidney disease in Japanese men. Hypertens Res 2008;31:485-92.
16. Heyden S, Borhani NO, Tyroler HA, Schneider KA, Langford HG, Hames CG, et al. The relationship of weight change to changes in blood pressure, serum uric acid, cholesterol and glucose in the treatment of hypertension. J Chronic Dis 1985;38:281-8.
17. Tsunoda S, Kamide K, Minami J, Kawano Y. Decreases in serum uric acid by amelioration of insulin resistance in overweight hypertensive patients: effect of a low-energy diet and an insulin-sensitizing agent. Am J Hypertens 2002;15:697-701.
18. Chiu KC, Cohan P, Lee NP, Chuang LM. Insulin sensitivity differs among ethnic groups with a compensatory response in beta-cell function. Diabetes Care 2000;23:1353-8.
19. Torrens JI, Skurnick J, Davidow AL, Korenman SG, Santoro N, Soto-Greene M, et al. Ethnic differences in insulin sensitivity and beta-cell function in premenopausal or early perimenopausal women without diabetes: the Study of Women's Health Across the Nation (SWAN). Diabetes Care 2004;27:354-61.
20. Retnakaran R, Hanley AJ, Connelly PW, Sermer M, Zinman B. Ethnicity modifies the effect of obesity on insulin resistance in pregnancy: a comparison of Asian, South Asian, and Caucasian women. J Clin Endocrinol Metab 2006;91:93-7.
21. Wingrove CS, Walton C, Stevenson JC. The effect of menopause on serum uric acid levels in non-obese healthy women. Metabolism 1998;47:435-8.
22. Hak AE, Choi HK. Menopause, postmenopausal hormone use and serum uric acid levels in US women — the Third National Health and Nutrition Examination Survey. Arthritis Res Ther 2008;10:R116.
23. Yahyaoui R, Esteva I, Haro-Mora JJ, Almaraz MC, Mordillo S, Rojo-Martinez G, et al. Effect of long-term administration of cross-sex hormone therapy on serum and urinary uric acid in transsexual persons. J Clin Endocrinol Metab 2008;93:2230-3.
24. Koga M, Saito H, Mukai M, Kasayama S, Yamamoto T. Factors contributing to increased serum urate in postmenopausal Japanese females. Climacteric 2009;12:146-52.
25. Ishizaka Y, Ishizaka N, Tani M, Toda A, Toda E, Koike K, et al. Association between changes in obesity parameters and incidence of chronic kidney disease in Japanese individuals. Kidney Blood Press Res 2009;32:141-9.
26. Sumino H, Ichikawa S, Kanda T, Nakamura T, Sakamaki T. Reduction of serum uric acid by hormone replacement therapy in postmenopausal women with hyperuricaemia. Lancet 1999;354:650.
27. Lofgren IE, Herron KL, West KL, Zern TL, Brownbill RA, Ilich

Table 3. Logistic regression analysis using the highest or lowest %dUA quartile as the dependent variable.

	Independent Variable			
	%dUA ≥ 7.2%		%dUA < −7.5%	
	OR (95% CI)	p	OR (95% CI)	p
Premenopausal women				
Model 1				
%dBMI quartile				
First			1.19 (0.73, 1.94)	0.474
2 and 3	1 Reference			
4	0.65 (0.42, 0.99)	0.046	1.00 Reference	
Model 2				
%dBMI quartile				
First			1.41 (0.85, 2.34)	0.181
2 and 3	1.00 Reference			
4	0.71 (0.45, 1.10)	0.126	1.00 Reference	
%deGFR	0.93 (0.91, 0.95)	< 0.001	1.06 (1.04, 1.08)	< 0.001
%dBPs	0.99 (0.97, 1.01)	0.225	1.00 (0.98, 1.02)	0.804
Postmenopausal women				
Model 1				
%dBMI quartile				
First			2.04 (1.37, 3.03)	< 0.001
2 and 3	1.00 Reference			
4	1.60 (1.06, 2.41)	0.025	1.00 Reference	
Model 2				
%dBMI				
First			2.04 (1.35, 3.07)	0.001
2 and 3	1.00 Reference			
4	1.72 (1.12, 2.63)	0.013	1.00 Reference	
%deGFR	0.95 (0.93, 0.97)	< 0.001	1.05 (1.03, 1.07)	< 0.001
%dBPs	0.98 (0.97, 1.00)	0.039	1.00 (0.98, 1.01)	0.684
Men				
Model 1				
%dBMI quartile				
First			1.35 (1.07, 1.69)	0.011
2 and 3	1.00 Reference			
4	1.38 (1.08, 1.76)	0.010	1.00 Reference	
Model 2				
%dBMI quartile				
First			1.46 (1.14, 1.86)	0.002
2 and 3	1.00 Reference			
4	1.49 (1.15, 1.92)	0.002	1.00 Reference	
%deGFR	0.94 (0.92, 0.95)	< 0.001	1.07 (1.06, 1.08)	< 0.001
%dBPs	1.00 (0.99, 1.01)	0.300	1.00 (0.99, 1.01)	0.715

Model 1. Independent variables include age, UA1, BMI1, and %dBMI quartiles. Model 2. Independent variables include Model 1 + %dBPs and %deGFR. UA: uric acid; BMI: body mass index; BPs: systolic blood pressure; eGFR: estimated glomerular filtration rate.

JZ, et al. Weight loss favorably modifies anthropometrics and reverses the metabolic syndrome in premenopausal women. J Am Coll Nutr 2005;24:486-93.

28. Matsuura F, Yamashita S, Nakamura T, Nishida M, Nozaki S, Funahashi T, et al. Effect of visceral fat accumulation on uric acid metabolism in male obese subjects: visceral fat obesity is linked more closely to overproduction of uric acid than subcutaneous fat obesity. Metabolism 1998;47:929-33.
29. Liberopoulos EN, Miltiadous GA, Elisaf MS. Alcohol intake, serum uric acid concentrations, and risk of gout. Lancet 2004;364:246-7; author reply 247.
30. Lain KY, Markovic N, Ness RB, Roberts JM. Effect of smoking on uric acid and other metabolic markers throughout normal pregnancy. J Clin Endocrinol Metab 2005;90:5743-6.

JOURNAL OF VIROLOGY, Mar. 2010, p. 2798–2807 Vol. 84, No. 6
0022-538X/10/$12.00 doi:10.1128/JVI.02499-09

Involvement of Ceramide in the Propagation of Japanese Encephalitis Virus▽

Hideki Tani, Mai Shiokawa, Yuuki Kaname, Hiroto Kambara, Yoshio Mori, Takayuki Abe, Kohji Moriishi, and Yoshiharu Matsuura*

Department of Molecular Virology, Research Institute for Microbial Diseases, Osaka University, Osaka, Japan

Received 27 November 2009/Accepted 22 December 2009

Japanese encephalitis virus (JEV) is a mosquito-borne RNA virus and one of the most important flaviviruses in the medical and veterinary fields. Although cholesterol has been shown to participate in both the entry and replication steps of JEV, the mechanisms of infection, including the cellular receptors of JEV, remain largely unknown. To clarify the infection mechanisms of JEV, we generated pseudotype (JEVpv) and recombinant (JEVrv) vesicular stomatitis viruses bearing the JEV envelope protein. Both JEVpv and JEVrv exhibited high infectivity for the target cells, and JEVrv was able to propagate and form foci as did authentic JEV. Anti-JEV envelope antibodies neutralized infection of the viruses. Treatment of cells with inhibitors for vacuolar ATPase and clathrin-mediated endocytosis reduced the infectivity of JEVpv, suggesting that JEVpv enters cells via pH- and clathrin-dependent endocytic pathways. Although treatment of the particles of JEVpv, JEVrv, and JEV with cholesterol drastically reduced the infectivity as previously reported, depletion of cholesterol from the particles by treatment with methyl β-cyclodextrin enhanced infectivity. Furthermore, treatment of cells with sphingomyelinase (SMase), which hydrolyzes membrane-bound sphingomyelin to ceramide, drastically enhanced infection with JEVpv and propagation of JEVrv, and these enhancements were inhibited by treatment with an SMase inhibitor or C_6-ceramide. These results suggest that ceramide plays crucial roles in not only entry but also egress processes of JEV, and they should assist in the clarification of JEV propagation and the development of novel therapeutics against diseases caused by infection with flaviviruses.

Japanese encephalitis virus (JEV) is a small, enveloped virus belonging to the family *Flaviviridae* and the genus *Flavivirus*, which also includes *Dengue virus* (DENV), *West Nile virus* (WNV), *Yellow fever virus*, and *Tick-borne encephalitis virus* (11). JEV is the most common agent of viral encephalitis, causing approximately 50,000 cases annually, of which 15,000 will die, and up to 50% of survivors are left with severe residual neurological complications. JEV has a single-stranded positive-sense RNA genome of approximately 11 kb, encoding a single large polyprotein, which is cleaved by the host- and virus-encoded proteases into three structural proteins, capsid (C), premembrane (PrM), and envelope (E), and seven nonstructural proteins. The structural proteins are components of viral particles, and the E protein is suggested to interact with a cell surface receptor molecule(s). Although a number of cellular components, including heat shock cognate protein 70 (33), glycosaminoglycans, such as heparin or heparan sulfate (21, 41), and laminin (3), have been shown to participate in JEV infection, the precise mechanisms by which these receptor candidates participate in JEV infection remain largely unclear.

In addition to the many studies identifying and characterizing receptor molecules in numerous viruses, data suggesting the involvement of membrane lipids, such as sphingolipids and cholesterol, in viral infection have also been accumulating. Lipid rafts consisting of sphingolipids and cholesterol and distributing to the outer leaflet of the cell membrane have been shown to be involved in the infection of not only many viruses but also several bacteria and parasites (24), in addition to playing roles in various functions such as lipid sorting, protein trafficking (26, 47), cell polarity, and signal transduction (38). With respect to cholesterol itself, various aspects of the life cycle of flaviviruses have been shown to involve this lipid, including the entry of DENV (34), hepatitis C virus (HCV) (16), and WNV (27), the membrane fusion of tick-borne encephalitis virus (40), and the replication of HCV (14, 17), WNV (23), and DENV (35). Recently Lee et al. (20) showed that treatment with cholesterol efficiently impairs both the entry and replication steps of JEV and DENV-2 but enhances infection with the Sindbis virus (22).

On the other hand, sphingolipids, including sphingomyelins and glycosphingolipids, are ubiquitous components of eukaryotic cell membrane structures, providing integrity to cellular membranes. Ceramide is one of the intermediates of sphingolipids and plays roles in cell differentiation, regulation of apoptosis and protein secretion, induction of cellular senescence, and other processes (2). Ceramide is generated from the hydrolysis of sphingomyelin by sphingomyelinase (SMase) or from catalysis by serine-palmitoyl-coenzyme A (CoA) transferase and ceramide synthase. Ceramide spontaneously self-associates to form ceramide-enriched microdomains and then to form larger ceramide-enriched membrane platforms which serve as the spatial and temporal organization for cellular signalosomes and for regulation of protein functions (2). The ceramide-enriched platforms have also been used by many pathogens to facilitate entry and infection (2). The acid SMase is activated not only by multiple stimuli, including receptor molecules, gamma irradiation, and some chemicals, but also by infection with some bacteria or viruses (36). Rhinovirus activates the SMase for generation of ceramide and forms ceramide-enriched membrane platforms that serve in the infection of

* Corresponding author. Mailing address: Department of Molecular Virology, Research Institute for Microbial Diseases, Osaka University, 3-1 Yamada-oka, Suita, Osaka 565-0871, Japan. Phone: 81-6-6879-8340. Fax: 81-6-6879-8269. E-mail: matsuura@biken.osaka-u.ac.jp.

▽ Published ahead of print on 6 January 2010.

target cells (10). Sindbis virus also activates the SMase and induces apoptosis through a continuous release of ceramide (15). In contrast to these viruses, ceramide inhibits infection with HIV (7) and HCV (48). Ceramide enrichment of the plasma membrane reduces expression of HCV receptor molecules through an ATP-independent internalization and impairs entry of HCV.

Pseudotype and recombinant viruses based on the vesicular stomatitis virus (VSV) bearing foreign viral envelope proteins have been shown to be powerful tools for the investigation of viral entry and the development of vaccines. These systems have been used to study infection with viruses that do not propagate readily (31, 43) or that are difficult to handle due to their high-level pathogenicity for humans (42). In addition, the systems allow us to focus on the investigation of entry mechanisms of particular viral envelope proteins by using control viruses harboring an appropriate protein on identical particles.

In the present study, we generated pseudotype (JEVpv) and recombinant (JEVrv) VSVs bearing the JEV envelope protein in human cell lines and determined the involvement of sphingolipids, especially ceramide, and cholesterol in infection of human cell lines with JEV. Both JEVpv and JEVrv exhibited infection of target cells via pH- and clathrin-dependent endocytosis. Treatment of cells with cholesterol impaired infection with JEVpv and JEVrv, as previously found in JEV infection (20). In contrast, treatment of cells with SMase drastically enhanced infection with both JEVpv and JEVrv and the production of infectious JEVrv particles. These results indicate that ceramide plays crucial roles in the entry and egress of JEV.

MATERIALS AND METHODS

Plasmids and cells. A cDNA clone encoding the PrM and E proteins of the AT31 strain was generated by PCR amplification, cloned into pCAGGS/MCS-PM (43), and designated pCAGC105E (JEV). The plasmid used for construction of JEVrv was pVSVΔG-GFP2.6 (provided by M. A. Whitt, University of Tennessee), which has additional transcription units with multicloning sites (MCS) and green fluorescent protein (GFP) located between the M and L genes. The PrM-E gene, obtained from pCAGC105E (JEV) by digestion with BglII and EcoRI, was cloned into the SmaI site of pVSVΔG-GFP2.6 after blunting, and the construct was designated pΔG-JEV (PrM-E). Huh7, BHK, Vero, and 293T cells were cultured in Dulbecco's modified Eagle's medium (DMEM) (Sigma, St. Louis, MO) containing 10% fetal bovine serum (FBS).

Viruses and chemicals. Wild-type JEV was used as described previously (29). The virus was amplified on Huh7 cells and stored at −80°C. The infectious titer was determined by using a focus-forming assay as described below. Bafilomycin A_1 from *Streptomyces griseus* was purchased from Fluka (Sigma). Chlorpromazine hydrochloride, sphingomyelinase (SMase), phospholipase C from *Bacillus cereus*, methyl-β-cyclodextrin (MβCD), a water-soluble cholesterol, and amitriptyline hydrochloride were obtained from Sigma. C_6-ceramide and sphingomyelin were purchased from Biomol International (Plymouth Meeting, PA). Biotin-ceramide was purchased from Echelon Biosciences Inc. (Salt Lake City, UT).

Reverse genetics of VSV. Recombinant VSVs were generated by a previously described method (43) with minor modifications. Briefly, BHK cells were grown to 90% confluence on 35-mm tissue culture plates and infected with a recombinant vaccinia virus encoding T7 RNA polymerase at a multiplicity of infection (MOI) of 5. After incubation at room temperature for 1 h, the cells were transfected with 4 μg of mixed plasmids encoding each component of VSV proteins (pBS-N/pBS-P/pBS-L/pBS-G, 3:5:1:8) and 2 μg of pΔG-Luci or pΔG-JEV (PrM-E) plasmid using the *Trans*IT-LT1 transfection reagent (Mirus, Madison, WI). After 48 h of incubation, the supernatants were passed through a filter with a pore size of 0.22 μm (Milex-GS; Millipore, Tokyo, Japan) to remove vaccinia virus and inoculated into 293T cells that had been transfected with pCAGVSVG (25) 24 h previously. Recovery of progeny virus was assessed by the appearance of cytopathic effects at 24 to 36 h postinfection. VSV G-complemented (*G) recombinant viruses were stored at −80°C. The infectious titers of the recovered viruses were determined by a plaque assay.

Production and characterization of JEVpv, JEVrv, and JEV. To generate JEVpv, Huh7 cells transiently expressing the PrM and E proteins by the transfection with pCAGC105E using *Trans*IT-LT1 (Mirus) were infected with VSVΔG/Luc-*G, in which the G gene was replaced with the luciferase gene and was pseudotyped with the G protein, at an MOI of 0.1. The virus was adsorbed for 2 h at 37°C and then extensively washed four times with serum-free DMEM. After 24 h of incubation at 37°C with 10% FBS-DMEM, the culture supernatants were centrifuged to remove cell debris and stored at −80°C. To generate JEVrv, Huh7 cells were infected with VSVΔG/JEV-*G at an MOI of 5 for 2 h at 37°C and then extensively washed four times with serum-free DMEM. After 24 h of incubation at 37°C with 10% FBS-DMEM, the culture supernatants were collected and stored at −80°C. Schematic representations of the genome structures and the production of recombinant and pseudotype VSVs are shown in Fig. 1. The purification and concentration of the pseudotype or recombinant viruses were conducted as described previously (43). Purified viruses and infected cell lysates were analyzed by immunoblotting to detect the incorporation of the envelope protein with anti-JEV E mouse polyclonal antibody (E#2-1; unpublished). The infectivities of JEVpv, JEVrv, and JEV were assessed by both luciferase activity and a focus-forming assay, as described below. The relative light unit (RLU) value of luciferase was determined by using the Bright-Glo luciferase assay system (Promega Corporation, Madison, WI), following a protocol provided by the manufacturer. To examine the effects of oligosaccharide modification of the JEV E protein in cells or on the particles, the cell lysates and the purified particles were digested with endoglycosidase H (Endo H) or peptide-N-glycosidase F (PNGase F) (Boehringer Mannheim, Mannheim, Germany), following a protocol provided by the manufacturer, and analyzed by immunoblotting.

Pseudotype VSVs bearing HCVE1E2 (HCVpv), VSVG (VSVpv), and murine leukemia virus envelope (MLVpv) proteins were produced in 293T cells transfected with pCAGc60-p7 (H77), pCAGVSVG, and pFBASALF (provided by T. Miyazawa, Kyoto University), respectively, and used as controls. Recombinant HCV (HCVrv) was also used as a control as described previously (43). To neutralize infection with JEVpv, JEVrv, and JEV, viruses were preincubated with the indicated dilution of anti-JEV E monoclonal antibody (22A1; provided by E. Konishi, Kobe University) for 1 h at 37°C and then inoculated into Huh7 cells. After 1 h of adsorption, the cells were washed three times with DMEM containing 10% FBS, and infectivity was determined after 24 h of incubation at 37°C.

Focus-forming assays. Cells infected with JEV, VSV, JEVrv, or HCVrv after treatment with the indicated reagents were cultured at 37°C with 0.8% methylcellulose in 10% FBS-DMEM for 24 or 48 h and fixed with 4% paraformaldehyde solution for 1 h. Cells were washed once with phosphate-buffered saline (PBS), treated with 0.5% Triton X-100 for 20 min for permeabilization, incubated with mouse monoclonal antibody to JEV (MsX Japanese encephalitis; Chemicon International Inc., Temecula, CA) for JEV or that to VSV N (10G4; provided by M. A. Whitt) for VSV, JEVrv, and HCVrv for 1 h, and stained by using a Vectastain Elite ABC anti-mouse IgG kit with a VIP substrate (Vector Laboratories, Burlingame, CA), following a protocol provided by the manufacturer.

Effects of chemicals on the infectivities of JEVpv, JEVrv, and JEV. To examine the entry pathways of the viruses, cells treated with various concentrations of bafilomycin A_1, chlorpromazine, MβCD, SMase, phospholipase C, or amitriptyline for 1 h at 37°C were inoculated with JEVpv, HCVpv, VSVpv, or MLVpv, and infectivity was determined by luciferase activity as described above. To examine the effects of cholesterol or SMase on the viral particles, purified virions incubated with various concentrations of water-soluble cholesterol or SMase for 1 h at 37°C were inoculated into the target cells. Viruses treated with SMase were ultracentrifuged (43) and resuspended in culture media to deplete any residual amount of SMase, and infectivity was determined by luciferase or focus-forming assay. To examine the effects of ceramide on the infection, 10 mM C_6-ceramide or sphingomyelin dissolved in ethanol was diluted with medium at various concentrations and preincubated with JEVpv, HCVpv, VSVpv, or MLVpv for 1 h at 37°C. After treatment, the viruses were inoculated into Huh7 cells, washed with medium after 1 h of incubation at 37°C, and cultured for 24 h at 37°C, and the residual infectivity was determined by measuring luciferase activity. The effects of C_6-ceramide on the infection of JEV were assessed by following the same protocol, and the residual infectivity was determined by focus-forming assay.

Ceramide binding assay. To examine the interaction of JEV E protein and ceramide, purified viruses were incubated with 500 μl of lysis buffer (20 mM Tris-HCl, pH 7.4, containing 135 mM NaCl and 1% Triton X-100) supplemented

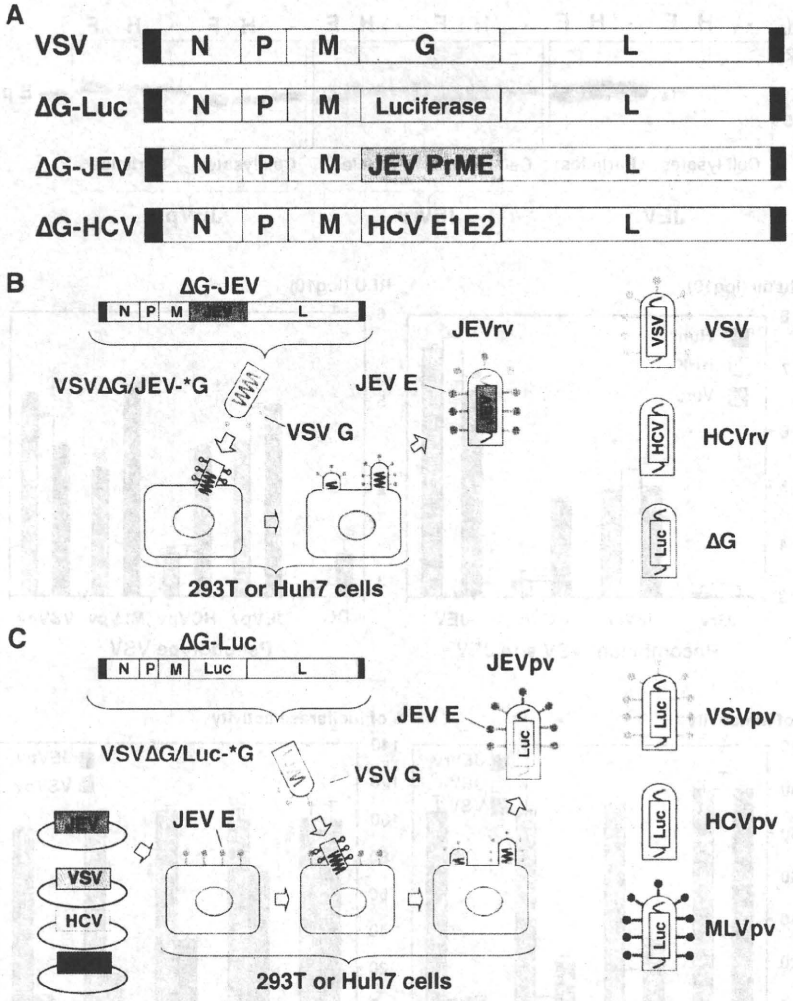

FIG. 1. Schematic representation of the genome structures and production of recombinant and pseudotype VSVs. (A) The luciferase, PrME, and E1E2 genes were inserted into the full-length cDNA clone of VSV in place of the G gene and designated ΔG-Luc, ΔG-JEV, and ΔG-HCV, respectively. (B) Recombinant VSVs, JEVrv, HCVrv, and ΔG, bearing the JEV E protein, HCV E1/E2 proteins, and no envelope, respectively, were generated in 293T or Huh7 cells by infection with the respective recombinant VSV after complementation with VSV G protein (*G). (C) Pseudotype VSVs, JEVpv, VSVpv, HCVpv, and MLVpv, were generated by infection with VSVΔG/Luc-*G in 293T or Huh7 cells transiently expressing the respective foreign protein.

with protease inhibitor cocktail (Roche, Indianapolis, IN) and 10 μl of 1-mg/ml biotin-ceramide in dimethyl sulfoxide (DMSO) for 1 h at 37°C, and then 20 μl of streptavidin-Sepharose 4B (Zymed, Invitrogen, Carlsbad, CA) was added and the solution was kept at 4°C for 4 h. After washing with the lysis buffer three times, the pellets were analyzed by immunoblotting with anti-JEV E polyclonal antibody (E#2-1).

RESULTS

Construction and characterization of recombinant and pseudotype VSVs. Recombinant VSVs were propagated in Huh7 cells by infection with VSVG-complemented (*G) recombinant VSVs possessing foreign genes of either JEV PrM/E, HCV E1/E2, or luciferase in place of the VSV G gene, as shown in Fig. 1A and B. The pseudotype VSVs, JEVpv, VSVpv, HCVpv, and MLVpv, were generated by infection with VSVΔG/Luc-*G in 293T or Huh7 cells transiently expressing the respective foreign protein (Fig. 1C).

To examine the properties of the JEV E proteins incorporated into JEV, JEVrv, and JEVpv particles, the E proteins expressed in Huh7 cells and incorporated into the viral particles were digested with Endo H or PNGase F and examined by immunoblotting (Fig. 2A). Although E proteins in the lysates of cells infected with JEV, JEVrv, or JEVpv were sensitive to both Endo H and PNGase F treatments, those incorporated into the viral particles were resistant to Endo H, suggesting that both JEVrv and JEVpv particles selectively incorporate the matured E proteins modified to the complex- or hybrid-type glycans as seen in the authentic JEV particles. Next, to examine the infectivity of JEVrv and JEVpv for the target cells, HCVpv, MLVpv, VSVpv, VSV, HCVrv, and ΔG were prepared as controls (Fig. 2B). Both JEVpv and JEVrv were infectious for Huh7, BHK, and Vero cells, whereas HCVpv and HCVrv were infectious for Huh7 cells but not for BHK

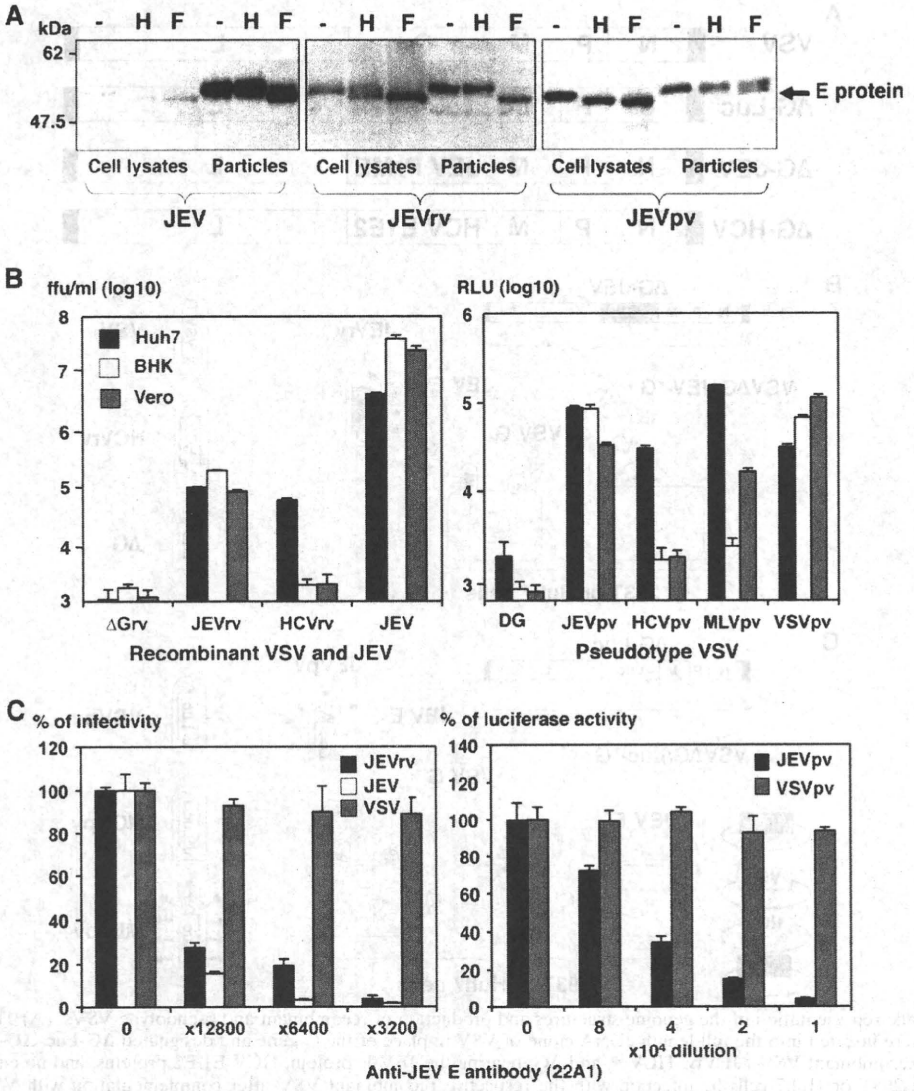

FIG. 2. Characterization of JEVrv and JEVpv. (A) JEV E proteins expressed in cells incorporated into the viral particles were treated with endoglycosidase H (H) or peptide-N-glycosidase F (F) and examined by immunoblotting using anti-E polyclonal antibody. "-" indicates an untreated sample. (B) Infectivities of recombinant viruses (left panel) and pseudotype viruses (right panel) were determined in Huh7, BHK, and Vero cells by a focus-forming assay and measurement of luciferase activity (RLU), respectively. VSV without envelope (ΔG) was used as a negative control. ffu, focus-forming units. (C) Neutralization of JEVrv (left panel) or JEVpv (right panel) infection by anti-E polyclonal antibody. Viruses were incubated with the indicated dilution of antibody for 1 h at room temperature and inoculated into Huh7 cells. Residual infectivities are expressed as percentages. VSV and VSVpv were used as controls. The results shown are from three independent assays, with error bars representing standard deviations.

and Vero cells, as previously reported (1). Although JEVpv and JEVrv generated in 293T cells were also infectious, these viruses were slightly more infective when generated in Huh7 cells, even though the efficiency of transfection of the expression plasmids into 293T cells was higher than that of transfection into Huh7 cells (data not shown). To determine the specificity of infection of JEVpv, JEVrv, and JEV, a neutralization assay was performed by using anti-E antibody (22A1). The infectivities of JEVpv and JEVrv but not of VSVpv and VSV for Huh7 cells were clearly inhibited by anti-E antibody in a dose-dependent manner (Fig. 2C). These results suggest that the JEVrv and JEVpv generated in this study had characteristics comparable to those of authentic JEV.

Entry pathways of JEVpv. Previous studies showed that JEV infection was inhibited by treatment with inhibitors of vacuolar acidification, such as ammonium chloride, concanamycin A, and bafilomycin A_1, suggesting that JEV enters target cells via pH-dependent endocytosis (30). Other flaviviruses, including WNV, DENV, and HCV, exhibit similar entry mechanisms (18, 45). To compare the entry pathway of JEV with those of other viruses, Huh7 cells were pretreated with various concentrations of bafilomycin A_1 and then the cells were inoculated

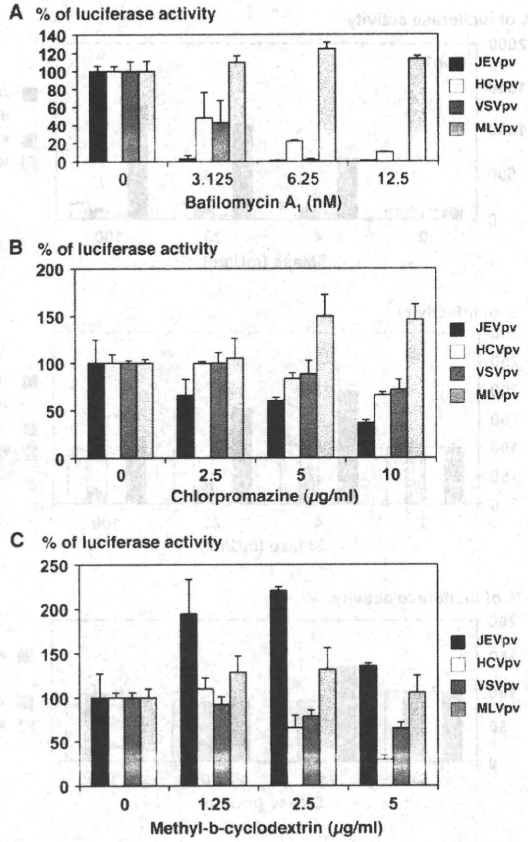

FIG. 3. Entry pathways of the pseudotype VSVs. Huh7 cells were pretreated with various concentrations of bafilomycin A_1 (A), chlorpromazine (B), or methyl-β-cyclodextrin (C) for 1 h and inoculated with the pseudotype viruses, JEVpv, HCVpv, VSVpv, and MLVpv. Luciferase activities were determined at 24 h postinfection. The results shown are from three independent assays, with error bars representing standard deviations.

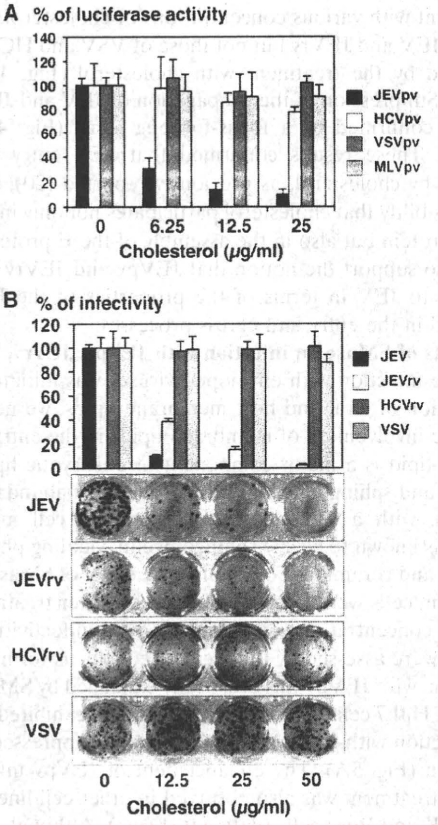

FIG. 4. Effects of cholesterol on infection with recombinant and pseudotype VSVs. (A) The pseudotype viruses were incubated with various concentrations of cholesterol for 1 h at room temperature and inoculated into Huh7 cells, and luciferase activities were determined at 24 h postinfection. (B) JEV, JEVrv, HCVrv, and VSV were incubated with various concentrations of cholesterol for 1 h at room temperature and inoculated into Huh7 cells, and residual infectivities were determined by focus-forming assay in a culture medium containing 1% methylcellulose at 48 h postinfection for JEV, JEVrv, and HCVrv and at 24 h postinfection for VSV. Foci of infected cells were detected by immunohistochemical staining (lower panel). The rate of focus formation of the viruses was analyzed by counting foci. The results shown are from three independent assays, with error bars representing standard deviations.

with JEVpv, HCVpv, VSVpv, and MLVpv (Fig. 3A). As expected, bafilomycin A_1 treatment did not affect the infectivity of MLVpv-bearing envelope proteins of MLV, which enters cells through a pH-independent direct fusion of the viral membrane and plasma membrane. In contrast, infections with HCVpv and VSVpv, which enter cells through pH-dependent endocytosis, were inhibited by treatment with bafilomycin A_1 in a dose-dependent manner. Similarly, infection with JEVpv was clearly inhibited by treatment with bafilomycin A_1 in a dose-dependent manner, suggesting that JEVpv enters cells through pH-dependent endocytosis, as seen in JEV infection.

To further examine the entry pathway of JEVpv, Huh7 cells were pretreated with various concentrations of chlorpromazine, an inhibitor of clathrin-mediated endocytosis, or MβCD, an inhibitor of caveolar/raft-mediated endocytosis, and infected with the pseudotype viruses. The infectivity of MLVpv was not affected by the treatment with either chlorpromazine or MβCD, as we expected. Treatment of cells with chlorpromazine slightly reduced the infectivity of JEVpv, HCVpv, and VSVpv in a dose-dependent manner (Fig. 3B), whereas treatment of cells with MβCD reduced the infectivity of HCVpv and VSVpv but increased the infectivity of JEVpv (Fig. 3C). These results suggest that JEVpv enters cells via clathrin-mediated endocytosis, as previously reported for infection with JEV (30), and that caveola/raft plays a different role in the entry of JEV than in the entry of HCV and VSV.

Effects of cholesterol on the entry and egress of JEV. Recently it was shown that entry of flaviviruses, including JEV and DENV, was drastically inhibited by treatment of the particles with cholesterol (20). To examine the effect of cholesterol on entry of JEV, the pseudotype viruses were inoculated into Huh7 cells after treatment with various concentrations of cholesterol. The infectivity of JEVpv but not that of HCVpv, VSVpv, or MLVpv was severely impaired by treatment with cholesterol in a dose-dependent manner (Fig. 4A). Next, to examine the effect of cholesterol on the propagation of JEV, the recombinant viruses were inoculated into Huh7 cells after

treatment with various concentrations of cholesterol. Infectivities of JEV and JEVrv but not those of VSV and HCVrv were inhibited by the treatment with cholesterol (Fig. 4B, upper panel). Suppression of the propagation of JEV and JEVrv was further confirmed by a focus-forming assay (Fig. 4B, lower panels). These results confirmed that JEV entry was suppressed by cholesterol, as previously reported (20), and raise the possibility that cholesterol participates not only in entry via the E protein but also in the assembly of the E protein. These data also support the notion that JEVpv and JEVrv are comparable to JEV in terms of the properties of the E protein involved in the entry and egress processes.

Effects of SMase on infection with JEVpv, JEVrv, and JEV. Because infection with enveloped viruses was initiated by the interaction of viral and host membrane lipids, we next examined the involvement of membrane lipids in the entry of JEV. Sphingolipid is a major component of eukaryotic lipid membranes, and sphingomyelin is one of the most abundant sphingolipids, with a wide presence across the cell membrane. SMase is known to cleave sphingomyelin, yielding phosphorylcholine and ceramide. To examine the effect of SMase on viral infection, cells were infected with viruses after treatment with various concentrations of SMase, and the infectivities of the viruses were assessed by the luciferase or focus-forming assay. Infection with JEVpv was drastically enhanced by SMase treatment of Huh7 cells, whereas such treatment exhibited no effect on infection with VSVpv and MLVpv and suppressed HCVpv infection (Fig. 5A). The enhancement of JEVpv infection by SMase treatment was also observed in other cell lines, including BHK and Vero cells (data not shown). Although the effect was not as evident as in JEVpv infection, SMase treatment exhibited a slight but substantial enhancement of the infectivity of JEV and JEVrv in Huh7 cells, in contrast to having no effect on VSV infection and a suppressive effect on HCVrv infection (Fig. 5B). The difference in the magnitude of enhancement of infectivity by treatment with SMase between infection with JEVpv and that with JEV or JEVrv might be attributable to the difference in the viral systems based on pseudotype (JEVpv) and replication-competent (JEV and JEVrv) viruses, which allow single and multiple rounds of infection, respectively. The effects of SMase may be more critical for the entry step than for other, later steps of infection. Suppression of HCVpv and HCVrv infection by treatment with SMase was consistent with previously reported data on infection of HCV-pseudotyped retroviral particles (HCVpp) and JFH1 virus (48).

Next, we examined the effect of SMase on the viral particles. Treatment of pseudotype particles of JEVpv, VSVpv, and MLVpv with various concentrations of SMase had no significant effect on their infectivity for Huh7 cells (Fig. 5C), whereas the infectivity of HCVpv particles was impaired by the treatment in a dose-dependent manner, as reported previously (1), suggesting that SMase treatment enhances the infectivity of JEVpv by modifying the molecules on target cells rather than the molecules on viral particles. To further determine the involvement of SMase in infection of JEVpv, cells were pretreated with various concentrations of amitriptyline, an inhibitor of acid SMase. The infectivity of JEVpv but not that of other viruses was decreased by the treatment with amitriptyline in a dose-dependent manner (Fig. 5D). A similar effect was observed with treatment with another SMase inhibitor, imipramine (data not shown). Collectively, these results suggest that entry of JEV into the target cells is enhanced by SMase treatment, which modifies the cell surface sphingolipids into a more competent state for interaction with the JEV envelope protein, thereby enabling its entry.

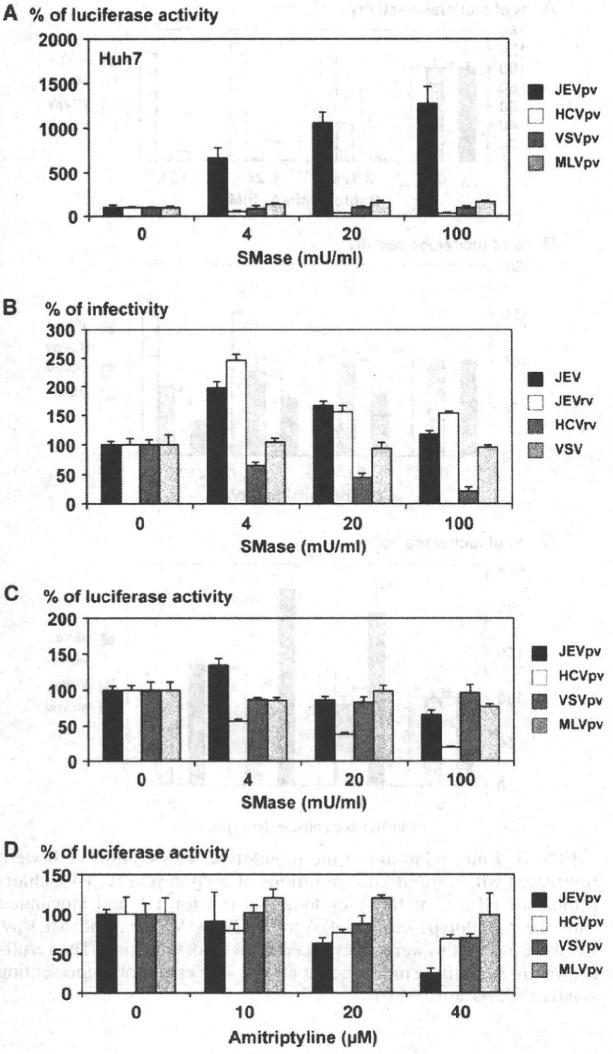

FIG. 5. Effects of SMase and amitriptyline treatment of cells on infection with pseudotype and recombinant VSVs. Huh7 cells were pretreated with various concentrations of SMase for 1 h, and then pseudotype viruses (A) or recombinant viruses (B) were inoculated. The infectivities were determined by luciferase activity measurement or focus-forming assay, and changes in infectivities are expressed as percentages. (C) The purified pseudotype particles were treated with various concentrations of SMase for 1 h and inoculated into Huh7 cells after removal of SMase by ultracentrifugation. Infectivities were determined at 24 h postinfection by measuring luciferase activity, and changes in infectivities are expressed as percentages. (D) Huh7 cells were pretreated with various concentrations of amitriptyline, an inhibitor for the acid SMase, for 1 h, and then pseudotype viruses were inoculated. Infectivities were determined at 24 h postinfection by measuring luciferase activity, and changes in infectivities are expressed as percentages. The results shown are from three independent assays, with error bars representing standard deviations.

Effects of SMase on propagation of JEVrv and JEV. We next examined the effects of SMase on the propagation of JEV. Recombinant VSV is capable of replicating by using the VSV genome and producing infectious particles bearing a foreign envelope protein encoded in place of the original G protein, and thus, it is feasible to assess the efficiency of not only entry but also egress of the recombinant viruses possessing foreign envelope genes of different origins, irrespective of their replication efficiency within the target cells. To examine the effects of SMase on viral propagation, cells were treated with various concentrations of the enzyme, inoculated with the recombinant viruses, and then cultured for up to 48 h in the presence of SMase. Production of JEVrv was dramatically enhanced by cultivation in the presence of SMase, in contrast to the suppression of HCVrv propagation (Fig. 6A). Although the effect of SMase treatment on the production of JEV was not as great as that seen in JEVrv propagation, treatment with SMase resulted in a substantial enhancement of JEV but not of VSV propagation (Fig. 6B). These results suggest that SMase treatment induces robust propagation of JEVrv mainly through enhancement of the entry step although also partly through enhancement of the egress step.

Involvement of ceramide in infection with JEV. Because treatment of cells with SMase induces production of ceramide, we next examined the effect of ceramide on the infectivity of the viruses. Treatment of the pseudotype particles with C_6-ceramide inhibited the infectivity of JEVpv for Huh7 cells in a dose-dependent manner, whereas no clear reduction of infectivity was observed with treatment of HCVpv, VSVpv, and MLVpv with ceramide (Fig. 7A). In contrast, treatment of the pseudotype particles with sphingomyelin, which is a substrate for SMase and is catalyzed into ceramide, did not affect the infectivity of the viruses, suggesting that the enhancement of infectivity of JEVpv by treatment with SMase was due to the generation of ceramide. Propagation of JEV but not of VSV was also suppressed by treatment of the viral particles with C_6-ceramide in a dose-dependent manner (Fig. 7B). Finally, to confirm the interaction of the JEV E protein with ceramide, purified JEV and JEVrv particles were incubated with biotin-ceramide and streptavidin-Sepharose 4B and examined by pull-down assay (Fig. 7C). The E proteins of both JEV and JEVrv were precipitated with the ceramide beads. These results indicate that the interaction of the JEV E protein with ceramide plays a crucial role in the entry of JEV.

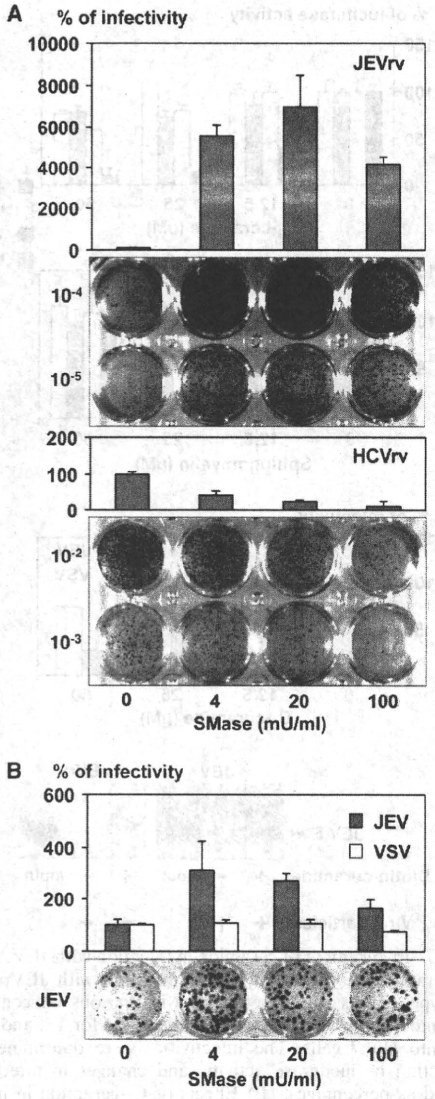

FIG. 6. Effects of SMase on the propagation of JEVrv and JEV. Huh7 cells were pretreated with various concentrations of SMase for 1 h and inoculated with JEVrv or HCVrv (A) or JEV or VSV (B), and infectivities were determined by focus-forming assay in a culture medium containing 1% methylcellulose at 48 h after infection with JEVrv, HCVrv, and JEV and at 24 h after infection with VSV. Titers were determined by counts of foci detected by immunohistochemical staining (lower panels). The results shown are from three independent assays, with error bars representing standard deviations.

DISCUSSION

Ceramide has been shown to play a crucial role in various cell signaling pathways through the clustering and activation of the receptor molecules in lipid rafts. Although the generation of ceramide inhibits the infectivity of HIV and HCV by the rearrangement of the entry receptor molecules (7, 48), rhinovirus and Sindbis virus generate ceramide by activating SMase for their entry and cell survival, respectively (10, 15). In this study, we demonstrated for the first time that ceramide plays crucial roles not only in the entry pathway of JEV but also in the egress through a direct interaction with the E envelope proteins.

To examine the roles of the E protein in the infectivity of JEV, we employed pseudotype and recombinant VSVs bearing JEV envelope proteins as surrogate systems in addition to authentic JEV. VSV assembles and buds from the plasma membrane, and therefore the surrogate viruses bearing the foreign envelope proteins being expressed on the plasma membrane exhibited more-efficient incorporation of the envelope proteins. Although the E protein of JEV, as well as that of other flaviviruses, including HCV, is mainly retained on the endoplasmic reticulum (ER) membrane, the E protein was incorporated into JEVpv and JEVrv particles and exhibited infectivity comparable to that of authentic JEV. Further studies are needed to clarify the mechanisms of incorporation of

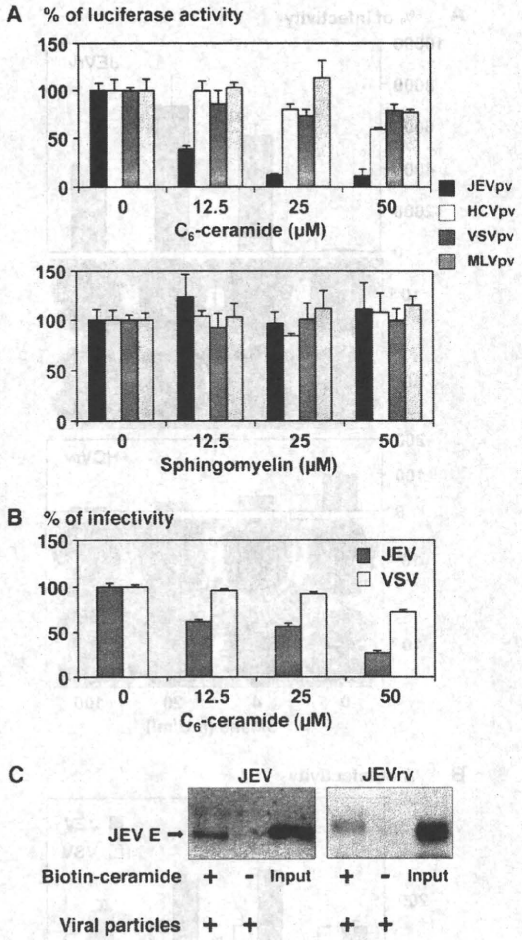

FIG. 7. Involvement of ceramide in infection with JEV. (A) Effects of C_6-ceramide or sphingomyelin in infection with JEVpv. Purified pseudotype viruses were pretreated with various concentrations of C_6-ceramide (upper) or sphingomyelin (lower) for 1 h and then inoculated into Huh7 cells. The infectivities were determined at 24 h postinfection by luciferase activity, and changes in infectivities are expressed as percentages. (B) Effects of C_6-ceramide in infection of JEVrv and JEV. JEV and VSV were pretreated with various concentrations of C_6-ceramide for 1 h, and then the viruses were inoculated into Huh7 cells. At 24 h postinfection, the infectivities were determined by focus-forming assay. (C) Binding of JEV and JEVrv to ceramide beads. Purified viruses were preincubated with (+) or without (−) biotin-ceramide resolved in DMSO and streptavidin-Sepharose 4B. After washing, residual pellets were analyzed by immunoblotting. Inputs are purified viruses. The results shown are from three independent assays, with error bars representing standard deviations.

the foreign envelope proteins on the ER membrane into VSV particles. In general, glycoproteins are modified into the complex type during the translocation from the ER to the Golgi apparatus. Although the JEV E glycoproteins were modified mainly into the high-mannose type in cells infected with JEVpv, JEVrv, or JEV, viruses possessing the E proteins were modified into the complex type within the particles. These results suggest that the E proteins of JEV and the surrogate viral particles are modified into the complex type after budding into the ER lumen during translocation into the Golgi apparatus. Recently assembly of DENV in the ER was revealed by three-dimensional architecture using electron tomography (49).

A number of viruses utilize cholesterol-rich membrane microdomains or lipid rafts for their entry, assembly, or egress processes (5). Cholesterol-rich membrane microdomains have been shown to be required for the entry but not for the replication of WNV through cholesterol depletion by treatment with MβCD (27). Entry of HCV was also shown to be partially required for cellular cholesterol (1, 16), which is consistent with the present data that infection with HCVpv was partially inhibited by treatment of cells with MβCD. Lee et al. recently reported that the infectivity of JEV, especially the replication step, was inhibited by treatment of cells with MβCD or the cholesterol chelation antibiotic filipin III (20). Furthermore, treatment of the viral particles with cholesterol inhibited the infectivity of JEV, in contrast to the enhancement of the infectivity of Sindbis virus by the same treatment (20, 22). Our data also indicated that the infectivity of JEVpv and JEVrv, as well as that of JEV, was completely inhibited by treatment of the particles with cholesterol in a dose-dependent manner, supporting the notion that the presence of an abundant amount of cholesterol increases the rigidity of the E protein of JEV particles and inhibits the membrane fusion event, as suggested by Lee et al. (20).

According to the current models, SMase alters the biophysical properties of the membrane bilayer by generating ceramide through the hydrolysis of sphingomyelin. Genetic disorders of SMase or ceramide metabolism are critically involved in human genetic diseases, such as Niemann-Pick disease (37) and Wilson's disease (19). *In vivo* studies of the function of SMase or ceramide in infections with pathogens are accumulating (9, 44, 46), and acid SMase-deficient mice have been shown to be unable to eliminate the pathogens because of failure to undergo apoptosis or phagolysosomal fusion, ultimately a massive release of cytokines and death by sepsis. It has recently been shown that acid SMase is a key regulator of cytotoxic granule secretion by primary T lymphocytes (13). The reduction of the cytolytic activity of $CD8^+$ cytotoxic T lymphocytes in acid SMase-deficient mice resulted in a significantly delayed clearance of lymphocytic choriomeningitis virus infection. Recently it was shown that entry of HCV is inhibited by SMase treatment through the downregulation of CD81, a major receptor of HCV, because enrichment of ceramide on the plasma membrane induces internalization of CD81 (48). HIV infection is also inhibited by ceramide enrichment through a restriction of the lateral diffusion of CD4 (6). Sindbis virus and rhinovirus activate the SMase and induce generation of ceramide in the endosomal membrane. Inhibition of SMase by genetic manipulation or pharmacological agents prevents infection with rhinoviruses, suggesting that SMase and ceramide-enriched membrane platforms play an important role in viral infection (10).

In this study, we have shown that entry of JEVpv, JEVrv, and JEV was specifically enhanced by treatment of cells with SMase. Treatment of cells with amitriptyline, an inhibitor interfering with the binding of SMase to the lipid bilayer, impaired the uptake of rhinovirus (10) and *Neisseria gonorrhoeae* (8). The entry of JEVpv was also inhibited by treatment with the inhibitor. Furthermore, the infections of JEVpv and JEV were inhibited by treatment with C_6-ceramide but not by treat-

ment with sphingomyelin, and JEV and JEVrv were coprecipitated with the ceramide beads, suggesting that the interaction of ceramide with the JEV E protein plays a crucial role in the early steps of infection. Ceramide is known to bind to the ceramide transport protein (CERT), which transports ceramide from the ER to the Golgi apparatus (12), and thus, it might be feasible to speculate that CERT participates in the translocation or maturation of the JEV E protein. Further studies are needed to clarify the interaction among ceramide, CERT, and the JEV E protein. Recently Aizaki et al. reported that the infectivity of HCV particles was decreased by treatment with MβCD or SMase, suggesting that cholesterols or sphingolipids incorporated into the virions are important for the infectivity of HCV (1). In this study, SMase treatment of HCVpv particles but not of JEVpv particles reduced infectivity, suggesting that incorporation of cholesterols and sphingolipids into the viral particles was different among flaviviruses.

The discrepancy between the drastic increase in the production of infectious particles of JEVrv and the marginal increase in that for JEV induced by SMase treatment in ceramide-enriched cells may indicate that ceramide enrichment enhances the entry and egress steps but negatively regulates genomic replication of JEV. Previously it was reported that digestion of sphingomyelin by SMase induces cholesterol redistribution (32), an increase in intracellular cholesterol esterification (4), and a decrease in cholesterol biosynthesis (39). Furthermore, ceramide has been shown to selectively displace cholesterol from lipid rafts and decrease the association of the cholesterol binding protein caveolin-1 (28, 50). Although we have not determined the cholesterol composition of the membranes of cells treated with SMase, cholesterol depletion induced by SMase treatment may also participate in the enhancement of JEV entry.

JEV initiates infection by interacting with receptor and/or coreceptor molecule(s), probably in cooperation with ceramide located in the ceramide-enriched platforms. The ceramide-enriched membrane domains facilitate signal transduction through reorganization and clustering of cell surface receptor molecules. Although the entry receptor(s) of JEV has not been well characterized yet, modification of the distribution, organization, and steric conformation of the receptor molecule(s) by treatment with SMase may facilitate entry of JEV. Generation of ceramide by SMase treatment has been shown to promote vesicular fusion processes and fusion of phagosomes, thereby engulfing bacteria with late endosomes and resulting in efficient intracellular bacterial killing (46).

In conclusion, we have demonstrated that the entry and egress processes of JEV were enhanced by treatment with SMase by using pseudotype and recombinant VSVs. The interaction of cellular ceramide and the E glycoproteins facilitates infection and propagation of JEV. Modification of sphingolipids on the plasma membrane of the target cells might be a novel target for the development of antivirals against JEV infection.

ACKNOWLEDGMENTS

We thank H. Murase for her secretarial work. We also thank M. A. Whitt and T. Miyazawa for providing plasmids and antibodies.

This research was supported in part by grants-in-aid from the Ministry of Health, Labor, and Welfare; the Ministry of Education, Culture, Sports, Science, and Technology; the Global Center of Excellence Program; and the Foundation for Biomedical Research and Innovation.

REFERENCES

1. **Aizaki, H., K. Morikawa, M. Fukasawa, H. Hara, Y. Inoue, H. Tani, K. Saito, M. Nishijima, K. Hanada, Y. Matsuura, M. M. Lai, T. Miyamura, T. Wakita, and T. Suzuki.** 2008. Critical role of virion-associated cholesterol and sphingolipid in hepatitis C virus infection. J. Virol. **82:**5715–5724.
2. **Bollinger, C. R., V. Teichgraber, and E. Gulbins.** 2005. Ceramide-enriched membrane domains. Biochim. Biophys. Acta **1746:**284–294.
3. **Boonsanay, V., and D. R. Smith.** 2007. Entry into and production of the Japanese encephalitis virus from C6/36 cells. Intervirology **50:**85–92.
4. **Chatterjee, S.** 1993. Neutral sphingomyelinase increases the binding, internalization, and degradation of low density lipoproteins and synthesis of cholesteryl ester in cultured human fibroblasts. J. Biol. Chem. **268:**3401–3406.
5. **Chazal, N., and D. Gerlier.** 2003. Virus entry, assembly, budding, and membrane rafts. Microbiol. Mol. Biol. Rev. **67:**226–237, table of contents.
6. **Finnegan, C. M., S. S. Rawat, E. H. Cho, D. L. Guiffre, S. Lockett, A. H. Merrill, Jr., and R. Blumenthal.** 2007. Sphingomyelinase restricts the lateral diffusion of CD4 and inhibits human immunodeficiency virus fusion. J. Virol. **81:**5294–5304.
7. **Finnegan, C. M., S. S. Rawat, A. Puri, J. M. Wang, F. W. Ruscetti, and R. Blumenthal.** 2004. Ceramide, a target for antiretroviral therapy. Proc. Natl. Acad. Sci. U. S. A. **101:**15452–15457.
8. **Grassme, H., E. Gulbins, B. Brenner, K. Ferlinz, K. Sandhoff, K. Harzer, F. Lang, and T. F. Meyer.** 1997. Acidic sphingomyelinase mediates entry of N. gonorrhoeae into nonphagocytic cells. Cell **91:**605–615.
9. **Grassme, H., V. Jendrossek, A. Riehle, G. von Kurthy, J. Berger, H. Schwarz, M. Weller, R. Kolesnick, and E. Gulbins.** 2003. Host defense against Pseudomonas aeruginosa requires ceramide-rich membrane rafts. Nat. Med. **9:**322–330.
10. **Grassme, H., A. Riehle, B. Wilker, and E. Gulbins.** 2005. Rhinoviruses infect human epithelial cells via ceramide-enriched membrane platforms. J. Biol. Chem. **280:**26256–26262.
11. **Gubler, D., G. Kuno, and L. Markoff.** 2007. Flaviviruses. p. 1153–1252. *In* D. M. Knipe and P. M. Howley (ed.), Fields virology, 5th ed., vol. 1. Lippincott-Williams & Wilkins, Philadelphia, PA.
12. **Hanada, K., K. Kumagai, S. Yasuda, Y. Miura, M. Kawano, M. Fukasawa, and M. Nishijima.** 2003. Molecular machinery for non-vesicular trafficking of ceramide. Nature **426:**803–809.
13. **Herz, J., J. Pardo, H. Kashkar, M. Schramm, E. Kuzmenkina, E. Bos, K. Wiegmann, R. Wallich, P. J. Peters, S. Herzig, E. Schmelzer, M. Kronke, M. M. Simon, and O. Utermohlen.** 2009. Acid sphingomyelinase is a key regulator of cytotoxic granule secretion by primary T lymphocytes. Nat. Immunol. **10:**761–768.
14. **Ikeda, M., K. Abe, M. Yamada, H. Dansako, K. Naka, and N. Kato.** 2006. Different anti-HCV profiles of statins and their potential for combination therapy with interferon. Hepatology **44:**117–125.
15. **Jan, J. T., S. Chatterjee, and D. E. Griffin.** 2000. Sindbis virus entry into cells triggers apoptosis by activating sphingomyelinase, leading to the release of ceramide. J. Virol. **74:**6425–6432.
16. **Kapadia, S. B., H. Barth, T. Baumert, J. A. McKeating, and F. V. Chisari.** 2007. Initiation of hepatitis C virus infection is dependent on cholesterol and cooperativity between CD81 and scavenger receptor B type I. J. Virol. **81:**374–383.
17. **Kapadia, S. B., and F. V. Chisari.** 2005. Hepatitis C virus RNA replication is regulated by host geranylgeranylation and fatty acids. Proc. Natl. Acad. Sci. U. S. A. **102:**2561–2566.
18. **Krishnan, M. N., B. Sukumaran, U. Pal, H. Agaisse, J. L. Murray, T. W. Hodge, and E. Fikrig.** 2007. Rab 5 is required for the cellular entry of dengue and West Nile viruses. J. Virol. **81:**4881–4885.
19. **Lang, P. A., M. Schenck, J. P. Nicolay, J. U. Becker, D. S. Kempe, A. Lupescu, S. Koka, K. Eisele, B. A. Klarl, H. Rubben, K. W. Schmid, K. Mann, S. Hildenbrand, H. Hefter, S. M. Huber, T. Wieder, A. Erhardt, D. Haussinger, E. Gulbins, and F. Lang.** 2007. Liver cell death and anemia in Wilson disease involve acid sphingomyelinase and ceramide. Nat. Med. **13:**164–170.
20. **Lee, C. J., H. R. Lin, C. L. Liao, and Y. L. Lin.** 2008. Cholesterol effectively blocks entry of flavivirus. J. Virol. **82:**6470–6480.
21. **Lee, E., and M. Lobigs.** 2002. Mechanism of virulence attenuation of glycosaminoglycan-binding variants of Japanese encephalitis virus and Murray Valley encephalitis virus. J. Virol. **76:**4901–4911.
22. **Lu, Y. E., T. Cassese, and M. Kielian.** 1999. The cholesterol requirement for Sindbis virus entry and exit and characterization of a spike protein region involved in cholesterol dependence. J. Virol. **73:**4272–4278.
23. **Mackenzie, J. M., A. A. Khromykh, and R. G. Parton.** 2007. Cholesterol manipulation by West Nile virus perturbs the cellular immune response. Cell Host Microbe **2:**229–239.
24. **Manes, S., G. del Real, and A. C. Martinez.** 2003. Pathogens: raft hijackers. Nat. Rev. Immunol. **3:**557–568.

25. **Matsuura, Y., H. Tani, K. Suzuki, T. Kimura-Someya, R. Suzuki, H. Aizaki, K. Ishii, K. Moriishi, C. S. Robison, M. A. Whitt, and T. Miyamura.** 2001. Characterization of pseudotype VSV possessing HCV envelope proteins. Virology **286:**263–275.
26. **Mayor, S., and H. Riezman.** 2004. Sorting GPI-anchored proteins. Nat. Rev. Mol. Cell Biol. **5:**110–120.
27. **Medigeshi, G. R., A. J. Hirsch, D. N. Streblow, J. Nikolich-Zugich, and J. A. Nelson.** 2008. West Nile virus entry requires cholesterol-rich membrane microdomains and is independent of alphavbeta3 integrin. J. Virol. **82:**5212–5219.
28. **Megha and E. London.** 2004. Ceramide selectively displaces cholesterol from ordered lipid domains (rafts): implications for lipid raft structure and function. J. Biol. Chem. **279:**9997–10004.
29. **Mori, Y., T. Yamashita, Y. Tanaka, Y. Tsuda, T. Abe, K. Moriishi, and Y. Matsuura.** 2007. Processing of capsid protein by cathepsin L plays a crucial role in replication of Japanese encephalitis virus in neural and macrophage cells. J. Virol. **81:**8477–8487.
30. **Nawa, M., T. Takasaki, K. Yamada, I. Kurane, and T. Akatsuka.** 2003. Interference in Japanese encephalitis virus infection of Vero cells by a cationic amphiphilic drug, chlorpromazine. J. Gen. Virol. **84:**1737–1741.
31. **Perez, M., R. Clemente, C. S. Robison, E. Jeetendra, H. R. Jayakar, M. A. Whitt, and J. C. de la Torre.** 2007. Generation and characterization of a recombinant vesicular stomatitis virus expressing the glycoprotein of Borna disease virus. J. Virol. **81:**5527–5536.
32. **Porn, M. I., and J. P. Slotte.** 1995. Localization of cholesterol in sphingomyelinase-treated fibroblasts. Biochem. J. **308**(Part 1)**:**269–274.
33. **Ren, J., T. Ding, W. Zhang, J. Song, and W. Ma.** 2007. Does Japanese encephalitis virus share the same cellular receptor with other mosquito-borne flaviviruses on the C6/36 mosquito cells? Virol. J. **4:**83.
34. **Reyes-Del Valle, J., S. Chavez-Salinas, F. Medina, and R. M. Del Angel.** 2005. Heat shock protein 90 and heat shock protein 70 are components of dengue virus receptor complex in human cells. J. Virol. **79:**4557–4567.
35. **Rothwell, C., A. Lebreton, C. Young Ng, J. Y. Lim, W. Liu, S. Vasudevan, M. Labow, F. Gu, and L. A. Gaither.** 2009. Cholesterol biosynthesis modulation regulates dengue viral replication. Virology **389:**8–19.
36. **Schenck, M., A. Carpinteiro, H. Grassme, F. Lang, and E. Gulbins.** 2007. Ceramide: physiological and pathophysiological aspects. Arch. Biochem. Biophys. **462:**171–175.
37. **Schuchman, E. H.** 2007. The pathogenesis and treatment of acid sphingomyelinase-deficient Niemann-Pick disease. J. Inherit. Metab. Dis. **30:**654–663.
38. **Simons, K., and D. Toomre.** 2000. Lipid rafts and signal transduction. Nat. Rev. Mol. Cell Biol. **1:**31–39.
39. **Slotte, J. P., and E. L. Bierman.** 1988. Depletion of plasma-membrane sphingomyelin rapidly alters the distribution of cholesterol between plasma membranes and intracellular cholesterol pools in cultured fibroblasts. Biochem. J. **250:**653–658.
40. **Stiasny, K., C. Koessl, and F. X. Heinz.** 2003. Involvement of lipids in different steps of the flavivirus fusion mechanism. J. Virol. **77:**7856–7862.
41. **Su, C. M., C. L. Liao, Y. L. Lee, and Y. L. Lin.** 2001. Highly sulfated forms of heparin sulfate are involved in Japanese encephalitis virus infection. Virology **286:**206–215.
42. **Takada, A., C. Robison, H. Goto, A. Sanchez, K. G. Murti, M. A. Whitt, and Y. Kawaoka.** 1997. A system for functional analysis of Ebola virus glycoprotein. Proc. Natl. Acad. Sci. U. S. A. **94:**14764–14769.
43. **Tani, H., Y. Komoda, E. Matsuo, K. Suzuki, I. Hamamoto, T. Yamashita, K. Moriishi, K. Fujiyama, T. Kanto, N. Hayashi, A. Owsianka, A. H. Patel, M. A. Whitt, and Y. Matsuura.** 2007. Replication-competent recombinant vesicular stomatitis virus encoding hepatitis C virus envelope proteins. J. Virol. **81:**8601–8612.
44. **Teichgraber, V., M. Ulrich, N. Endlich, J. Riethmuller, B. Wilker, C. C. De Oliveira-Munding, A. M. van Heeckeren, M. L. Barr, G. von Kurthy, K. W. Schmid, M. Weller, B. Tummler, F. Lang, H. Grassme, G. Doring, and E. Gulbins.** 2008. Ceramide accumulation mediates inflammation, cell death and infection susceptibility in cystic fibrosis. Nat. Med. **14:**382–391.
45. **Tscherne, D. M., C. T. Jones, M. J. Evans, B. D. Lindenbach, J. A. McKeating, and C. M. Rice.** 2006. Time- and temperature-dependent activation of hepatitis C virus for low-pH-triggered entry. J. Virol. **80:**1734–1741.
46. **Utermohlen, O., J. Herz, M. Schramm, and M. Kronke.** 2008. Fusogenicity of membranes: the impact of acid sphingomyelinase on innate immune responses. Immunobiology **213:**307–314.
47. **Viola, A., and N. Gupta.** 2007. Tether and trap: regulation of membrane-raft dynamics by actin-binding proteins. Nat. Rev. Immunol. **7:**889–896.
48. **Voisset, C., M. Lavie, F. Helle, A. Op De Beeck, A. Bilheu, J. Bertrand-Michel, F. Terce, L. Cocquerel, C. Wychowski, N. Vu-Dac, and J. Dubuisson.** 2008. Ceramide enrichment of the plasma membrane induces CD81 internalization and inhibits hepatitis C virus entry. Cell Microbiol. **10:**606–617.
49. **Welsch, S., S. Miller, I. Romero-Brey, A. Merz, C. K. Bleck, P. Walther, S. D. Fuller, C. Antony, J. Krijnse-Locker, and R. Bartenschlager.** 2009. Composition and three-dimensional architecture of the dengue virus replication and assembly sites. Cell Host Microbe. **5:**365–375.
50. **Yu, C., M. Alterman, and R. T. Dobrowsky.** 2005. Ceramide displaces cholesterol from lipid rafts and decreases the association of the cholesterol binding protein caveolin-1. J. Lipid Res. **46:**1678–1691.

JOURNAL OF VIROLOGY, June 2010, p. 5824–5835 Vol. 84, No. 11
0022-538X/10/$12.00 doi:10.1128/JVI.02397-09

Production of Infectious Hepatitis C Virus by Using RNA Polymerase I-Mediated Transcription▽

Takahiro Masaki,[1]† Ryosuke Suzuki,[1]† Mohsan Saeed,[1,4] Ken-ichi Mori,[2] Mami Matsuda,[1] Hideki Aizaki,[1] Koji Ishii,[1] Noboru Maki,[2] Tatsuo Miyamura,[1] Yoshiharu Matsuura,[3] Takaji Wakita,[1] and Tetsuro Suzuki[1]*

Department of Virology II, National Institute of Infectious Diseases, Shinjuku-ku, Tokyo 162-8640, Japan[1]; Advanced Life Science Institute, Wako, Saitama 351-0112, Japan[2]; Department of Molecular Virology, Research Institute for Microbial Diseases, Osaka University, Suita-shi, Osaka 565-0871, Japan[3]; and Graduate School of Medicine, The University of Tokyo, Tokyo 113-0033, Japan[4]

Received 13 November 2009/Accepted 8 March 2010

In this study, we used an RNA polymerase I (Pol I) transcription system for development of a reverse genetics protocol to produce hepatitis C virus (HCV), which is an uncapped positive-strand RNA virus. Transfection with a plasmid harboring HCV JFH-1 full-length cDNA flanked by a Pol I promoter and Pol I terminator yielded an unspliced RNA with no additional sequences at either end, resulting in efficient RNA replication within the cytoplasm and subsequent production of infectious virions. Using this technology, we developed a simple replicon *trans*-packaging system, in which transient transfection of two plasmids enables examination of viral genome replication and virion assembly as two separate steps. In addition, we established a stable cell line that constitutively produces HCV with a low mutation frequency of the viral genome. The effects of inhibitors of N-linked glycosylation on HCV production were evaluated using this cell line, and the results suggest that certain step(s), such as virion assembly, intracellular trafficking, and secretion, are potentially up- and downregulated according to modifications of HCV envelope protein glycans. This Pol I-based HCV expression system will be beneficial for a high-throughput antiviral screening and vaccine discovery programs.

Over 170 million people worldwide have been infected with hepatitis C virus (HCV) (22, 33, 37), and persistence of HCV infection is one of the leading causes of liver diseases, such as chronic hepatitis, cirrhosis, and hepatocellular carcinoma (16, 25, 38). The HCV genome is an uncapped 9.6-kb positive-strand RNA sequence consisting of a 5′ untranslated region (UTR), an open reading frame encoding at least 10 viral proteins (Core, E1, E2, p7, NS2, NS3, NS4A, NS4B, NS5A, and NS5B), and a 3′UTR (46). The structural proteins (Core, E1, and E2) reside in the N-terminal region.

The best available treatment for HCV infection, which is pegylated alpha interferon (IFN-α) combined with ribavirin, is effective in only about half of patients and is often difficult to tolerate (25). To date, a prophylactic or therapeutic vaccine is not available. There is an urgent need to develop more effective and better tolerated therapies for HCV infection. Recently, a robust system for HCV production and infection in cultured cells has been developed. The discovery that some HCV isolates can replicate in cell cultures and release infectious particles has allowed the complete viral life cycle to be studied (23, 49, 53). The most robust system for HCV production involves transfection of Huh-7 cells with genomic HCV RNA of the JFH-1 strain by electroporation. However, using this RNA transfection system, the amount of secreted infectious viruses often fluctuate and mutations emerge in HCV genome with multiple passages for an extended period of time (54), which limits its usefulness for antiviral screening and vaccine development.

DNA-based expression systems for HCV replication and virion production have also been examined (5, 15, 21). With DNA-based expression systems, transcriptional expression of functional full-length HCV RNA is controlled by an RNA polymerase II (Pol II) promoter and a self-cleaving ribozyme(s). DNA expression systems using RNA polymerase I (Pol I) have been utilized in reverse genetics approaches to replicate negative-strand RNA viruses, including influenza virus (12, 29), Uukuniemi virus (11), Crimean-Congo hemorrhagic fever virus (10), and Ebola virus (13). Pol I is a cellular enzyme that is abundantly expressed in growing cells and transcribes rRNA lacking both a 5′ cap and a 3′ poly(A) tail. Thus, viral RNA synthesized in cells transfected with Pol I-driven plasmids containing viral genomic cDNA has no additional sequences at the 5′- or 3′ end even in the absence of a ribozyme sequence (28). The advantages of DNA-based expression systems are that DNA expression plasmids are easier to manipulate and generate stable cell lines that constitutively express the viral genome.

We developed here a new HCV expression system based on transfection of an expression plasmid containing a JFH-1 cDNA clone flanked by Pol I promoter and terminator sequences to generate infectious HCV particles from transfected cells. The technology presented here has strong potential to be the basis for *trans*-encapsidation system by transient transfection of two plasmids and for the establishment of an efficient and reliable screening system for potential antivirals.

MATERIALS AND METHODS

DNA construction. To generate HCV-expressing plasmids containing full-length JFH1 cDNA embedded between Pol I promoter and terminator se-

* Corresponding author. Present address: Department of Infectious Diseases, Hamamatsu University School of Medicine, Hamamatsu 431-3192, Japan. Phone: 81-53-435-2336. Fax: 81-53-435-2337. E-mail: tesuzuki@hama-med.ac.jp.

† T.M. and R.S. contributed equally to this study.

▽ Published ahead of print on 17 March 2010.

quences, part of the 5′UTR region and part of the NS5B to the 3′UTR region of full-length JFH-1 cDNA were amplified by PCR using primers containing BsmBI sites. Each amplification product was then cloned into a pGEM-T Easy vector (Promega, Madison, WI) and verified by DNA sequencing. Both fragments were excised by digestion with NotI and BsmBI, after which they were cloned into the BsmBI site of the pHH21 vector (a gift from Yoshihiro Kawaoka, School of Veterinary Medicine, University of Wisconsin-Madison [29]), which contains a human Pol I promoter and a mouse Pol I terminator. The resultant plasmid was digested by AgeI and EcoRV and ligated to JFH-1 cDNA digested by AgeI and EcoRV to produce pHHJFH1. pHHJFH1/GND having a point mutation at the GDD motif in NS5B to abolish RNA-dependent RNA polymerase activity and pHHJFH1/R783A/R785A carrying double Arg-to-Ala substitutions in the cytoplasmic loop of p7 were constructed by oligonucleotide-directed mutagenesis. To generate pHHJFH1/ΔE carrying in-frame deletions of parts of the E1 and E2 regions (amino acids [aa] 256 to 567), pHHJFH1 was digested with NcoI and AscI, followed by Klenow enzyme treatment and self-ligation. To generate pHH/SGR-Luc carrying the bicistronic subgenomic HCV reporter replicon and its replication-defective mutant, pHH/SGR-Luc/GND, AgeI-SpeI fragments of pHHJFH1 and pHHJFH1/GND were replaced with an AgeI-SpeI fragment of pSGR-JFH1/Luc (20). In order to construct pCAG/C-NS2 and pCAG/C-p7, PCR-amplified cDNA for C-NS2 and C-p7 regions of the JFH-1 strain were inserted into the EcoRI sites of pCAGGS (30). In order to construct stable cell lines, a DNA fragment containing a Zeocin resistance gene excised from pSV2/Zeo2 (Invitrogen, Carlsbad, CA) was inserted into pHH21 (pHHZeo). Full-length JFH-1 cDNA was then inserted into the BsmBI sites of pHHZeo. The resultant construct was designated pHHJFH1/Zeo.

Cells and compounds. The human hepatoma cell line, Huh-7, and its derivative cell line, Huh7.5.1 (a gift from Francis V. Chisari, The Scripps Research Institute), were maintained in Dulbecco modified Eagle medium (DMEM) supplemented with nonessential amino acids, 100 U of penicillin/ml, 100 μg of streptomycin/ml, and 10% fetal bovine serum (FBS) at 37°C in a 5% CO_2 incubator. *N*-Nonyl-deoxynojirimycin (*N*N-DNJ) and kifunensine (KIF) were purchased from Toronto Research Chemicals (Ontario, Canada), castanospermine (CST) and 1,4-dideoxy-1,4-imino-D-mannitol hydrochloride (DIM) were from Sigma-Aldrich (St. Louis, MO), 1-deoxymannojirimycin (DMJ) and swainsonine (SWN) were from Alexis Corp. (Lausen, Switzerland), and *N*-butyldeoxynojirimycin (*N*B-DNJ) was purchased from Wako Chemicals (Osaka, Japan). BILN 2061 was a gift from Boehringer Ingelheim (Canada), Ltd. These compounds were dissolved in dimethyl sulfoxide and used for the experiments. IFN-α was purchased from Dainippon-Sumitomo (Osaka, Japan).

DNA transfection and selection of stable cell lines. DNA transfection was performed by using FuGENE 6 transfection reagent (Roche, Mannheim, German) in accordance with the manufacturer's instructions. To establish stable cell lines constitutively producing HCV particles, pHHJFH1/Zeo was transfected into Huh7.5.1 cells within 35-mm dishes. At 24 h posttransfection (p.t.), the cells were then divided into 100-mm dishes at various cell densities and incubated with DMEM containing 0.4 mg of zeocin/ml for approximately 3 weeks. Selected cell colonies were picked up and amplified. The expression of HCV proteins was confirmed by measuring secreted core proteins. The stable cell line established was designated H751JFH1/Zeo.

***In vitro* synthesis of HCV RNA and RNA transfection.** RNA synthesis and transfection were performed as previously described (26, 49).

RNA preparation, Northern blotting, and RNase protection assay (RPA). Total cellular RNA was extracted with a TRIzol reagent (Invitrogen), and HCV RNA was isolated from filtered culture supernatant by using the QIAamp viral RNA minikit (Qiagen, Valencia, CA). Extracted cellular RNA was treated with DNase (TURBO DNase; Ambion, Austin, TX) and cleaned up by using an RNeasy minikit, which includes another step of RNase-free DNase digestion (Qiagen). The cellular RNA (4 μg) was separated on 1% agarose gels containing formaldehyde and transferred to a positively charged nylon membrane (GE Healthcare, Piscataway, NJ). After drying and cross-linking by UV irradiation, hybridization was performed with [α-^{32}P]dCTP-labeled DNA using Rapid-Hyb buffer (GE Healthcare). The DNA probe was synthesized from full-length JFH-1 cDNA using the Megaprime DNA labeling system (GE Healthcare). Quantification of positive- and negative-strand HCV RNA was performed using the RPA with biotin-16-uridine-5′-triphosphate (UTP)-labeled HCV-specific RNA probes, which contain 265 nucleotides (nt) complementary to the positive-strand (+) 5′UTR and 248 nt complementary to the negative-strand (−) 3′UTR. Human β-actin RNA probes labeled with biotin-16-UTP were used as a control to normalize the amount of total RNA in each sample. The RPA was carried out using an RPA III kit (Ambion) according to the manufacturer's procedures. Briefly, 15 μg of total cellular RNA was used for hybridization with 0.3 ng of the β-actin probe and 0.6 ng of either the HCV (+) 5′UTR or (−) 3′UTR RNA probe. After digestion with RNase A/T1, the RNA products were analyzed by electrophoresis in a 6% polyacrylamide–8 M urea gel and visualized by using a chemiluminescent nucleic acid detection module (Thermo Scientific, Rockford, IL) according to the manufacturer's instructions.

Reverse transcriptase PCR (RT-PCR), sequencing, and rapid amplification of cDNA ends (RACE). Aliquots (5 μl) of RNA solution extracted from filtered culture supernatant were subjected to reverse transcription with random hexamer and Superscript II reverse transcriptase (Invitrogen). Four fragments of HCV cDNA (nt 129 to 2367, nt 2285 to 4665, nt 4574 to 7002, and nt 6949 to 9634), which covers most of the HCV genome, were amplified by nested PCR. Portions (1 or 2 μl) of each cDNA sample were subjected to PCR with TaKaRa LA *Taq* polymerase (Takara, Shiga, Japan). The PCR conditions consisted of an initial denaturation at 95°C for 2 min, followed by 30 cycles of denaturation at 95°C for 30 s, annealing at 60°C for 30 s, and extension at 72°C for 3 min. The amplified products were separated by agarose gel electrophoresis and used for direct DNA sequencing. To establish the 5′ ends of the HCV transcripts from pHHJFH1, a synthetic 45-nt RNA adapter (Table 1) was ligated to RNA extracted from the transfected cells 1 day p.t. using T4 RNA ligase (Takara). The viral RNA sequences were then reverse transcribed using SuperScript III reverse transcriptase (Invitrogen) with a primer, RT (Table 1). The resultant cDNA sequences were subsequently amplified by PCR with 5′RACEouter-S and 5′RACEouter-R primers, followed by a second cycle of PCR using 5′RACEinner-S and 5′RACEinner-R primers (Table 1). To establish the terminal 3′-end sequences, extracted RNA sequences were polyadenylated using a poly(A) polymerase (Takara), reverse transcribed with CAC-T35 primer (Table 1), and amplified with the primers 3X-10S (Table 1) and CAC-T35. The amplified 5′ and 3′ cDNA sequences were then separated by agarose gel electrophoresis, cloned into the pGEM-T Easy vector (Promega), and sequenced.

Western blotting. The proteins were transferred onto a polyvinylidene difluoride membrane (Immobilon; Millipore, Bedford, MA) after separation by SDS-PAGE. After blocking, the membranes were probed with a mouse monoclonal anti-HCV core antibody (2H9) (49), a rabbit polyclonal anti-NS5B antibody, or a mouse monoclonal GAPDH (glyceraldehyde-3-phosphate dehydrogenase) antibody (Chemicon, Temecula, CA), followed by incubation with a peroxidase-conjugated secondary antibody and visualization with an ECL Plus Western blotting detection system (Amersham, Buckinghamshire, United Kingdom).

Quantification of HCV core protein. HCV core protein was quantified by using a highly sensitive enzyme immunoassay (Ortho HCV antigen ELISA kit; Ortho Clinical Diagnostics, Tokyo, Japan) in accordance with the manufacturer's instructions.

Sucrose density gradient analysis. Samples of cell culture supernatant were processed by low-speed centrifugation and passage through a 0.45-μm-pore-size filter. The filtrated supernatant was then concentrated ~30-fold by ultrafiltration by using an Amicon Ultra-15 filter device with a cutoff molecular mass of 100,000 kDa (Millipore), after which it was layered on top of a continuous 10 to 60% (wt/vol) sucrose gradient, followed by centrifugation at 35,000 rpm at 4°C for 14 h with an SW41 rotor (Beckman Coulter, Fullerton, CA). Fractions of 1 ml were collected from the bottom of the gradient. The core level and infectivity of HCV in each fraction were determined.

Quantification of HCV infectivity. Infectious virus titration was performed by a 50% tissue culture infectious dose ($TCID_{50}$) assay, as previously described (23, 26). Briefly, naive Huh7.5.1 cells were seeded at a density of 10^4 cells/well in a 96-well flat-bottom plate 24 h prior to infection. Five serial dilutions were performed, and the samples were used to infect the seeded cells (six wells per dilution). At 72 h after infection, the inoculated cells were fixed and immunostained with a rabbit polyclonal anti-NS5A antibody (14), followed by an Alexa Fluor 488-conjugated anti-rabbit secondary antibody (Invitrogen).

Labeling of *de novo*-synthesized viral RNA and immunofluorescence staining. Labeling of *de novo*-synthesized viral RNA was performed as previously described with some modifications (40). Briefly, cells were plated onto an eight-well chamber slide at a density of 5×10^4 cells/well. One day later, the cells were incubated with actinomycin D at a final concentration of 10 μg/ml for 1 h and washed twice with HEPES-saline buffer. Bromouridine triphosphate (BrUTP) at 2 mM was subsequently transfected into the cells using FuGENE 6 transfection reagent, after which the cells were incubated for 15 min on ice. After the cells were washed twice with phosphate-buffered saline (PBS), they were incubated in fresh DMEM supplemented with 10% FBS at 37°C for 4 h. The cells were then fixed with 4% paraformaldehyde for 20 min and permeabilized with PBS containing 0.1% Triton X-100 for 15 min at room temperature. Immunofluorescence staining of NS5A and *de novo*-synthesized HCV RNA was performed as previously described (26, 40). The nuclei were stained with DAPI (4′,6′-diamidino-2-phenylindole) solution (Sigma-Aldrich). Confocal microscopy was performed

TABLE 1. Oligonucleotides used for RT-PCR and RACE of the JFH-1 genome

Method or segment	Oligonucleotide	Sequences (5′–3′)
5′RACE	RT	GTACCCCATGAGGTCGGCAAAG
	45-nt RNA adapter	GCUGAUGGCGAUGAAUGAACACUGCGUUUGCUGGCUUUGAUGAAA
	5′RACEouter-S	GCTGATGGCGATGAATGAACACTG
	5′RACEouter-R	GACCGCTCCGAAGTTTTCCTTG
	5′RACEinner-S	GAACACTGCGTTTGCTGGCTTTGATG
	5′RACEinner-R	CGCCCTATCAGGCAGTACCACAAG
3′RACE	CAC-T35	CACTTTTTTTTTTTTTTTTTTTTTTTTTTTTTTTTT
	3X-10S	ATCTTAGCCCTAGTCACGGC
nt 129-2367	44S (1st PCR)	CTGTGAGGAACTACTGTCTT
	2445R	TCCACGATGTTCTGGTGAAG
	17S (2nd PCR)	CGGGAGAGCCATAGTGG
	2367R	CATTCCGTGGTAGAGTGCA
nt 2285-4665	2099S (1st PCR)	ACGGACTGTTTTAGGAAGCA
	4706R	TTGCAGTCGATCACGGAGTC
	2285S (2nd PCR)	AACTTCACTCGTGGGGATCG
	4665R	TCGGTGGCGACGACCAC
nt 4574-7002	4547S (1st PCR)	AAGTGTGACGAGCTCGCGG
	7027R	CATGAACAGGTTGGCATCCACCAT
	4594S (2nd PCR)	CGGGGTATGGGCTTGAACGC
	7003R	GTGGTGCAGGTGGCTCGCA
nt 6949-9634	6881S (1st PCR)	ATTGATGTCCATGCTAACAG
	3X-75R	TACGGCACTCTCTGCAGTCA
	6950S (2nd PCR)	GAGCTCCTCAGTGAGCCAG
	3X-54R	GCGGCTCACGGACCTTTCAC

using a Zeiss confocal laser scanning microscope LSM 510 (Carl Zeiss, Oberkochen, Germany).

Luciferase assay. Huh7.5.1 cells were seeded onto a 24-well cell culture plate at a density of 3×10^4 cells/well 24 h prior to inoculation with 100 μl of supernatant from the transfected cells. The cells were incubated for 72 h, followed by lysis with 100 μl of lysis buffer. The luciferase activity of the cells was determined by using a luciferase assay system (Promega). All luciferase assays were done at least in triplicate. For the neutralization experiments, a mouse monoclonal anti-CD81 antibody (JS-81; BD Pharmingen, Franklin Lakes, NJ) and a mouse monoclonal anti-FLAG antibody (Sigma-Aldrich) were used.

Flow cytometric analysis. Cells detached by treatment with trypsin were incubated in PBS containing 1% (vol/vol) formaldehyde for 15 min. A total of 5×10^5 cells were resuspended in PBS and treated with or without 0.75 μg of anti-CD81 antibody for 30 min at 4°C. After being washed with PBS, the cells were incubated with an Alexa Fluor 488-conjugated anti-mouse secondary antibody (Invitrogen) at 1:200 for 30 min at 4°C, washed repeatedly, and resuspended in PBS. Analyses were performed by using FACSCalibur system (Becton Dickinson, Franklin Lakes, NJ).

RESULTS

Analysis of the 5′ and 3′ ends of HCV RNA sequences generated from Pol I-driven plasmids. To examine whether the HCV transcripts generated from Pol I-driven plasmids had correct nucleotides at the 5′ and 3′ ends, we extracted RNA from Huh-7 cells transfected with pHHJFH1, which carries a genome-length HCV cDNA with a Pol I promoter/terminator, as well as from the culture supernatants. After this, the nucleotide sequences at both ends were determined using RACE and sequence analysis. A 328-nt fragment corresponding to cDNA from the 5′ end of HCV RNA was detected in the cell samples (Fig. 1A). Cloning of amplified fragments confirmed that the HCV transcripts were initiated from the first position of the viral genome in all of the clones sequenced (Fig. 1B). Similarly, a 127-nt amplification fragment was detected in each sample by 3′RACE (Fig. 1C), and the same 3′-end nucleotide sequence was observed in all clones derived from the culture supernatant (Fig. 1D, left). An additional two nucleotides (CC) were found at the 3′ end of the HCV transcript in a limited number of sequences (1 of 11 clones) derived from the cell sample (Fig. 1D, right), which were possibly derived from the Pol I terminator sequence by incorrect termination. These results indicate that most HCV transcripts generated from the Pol I-based HCV cDNA expression system are faithfully processed, although it is not determined whether the 5′ terminus of the viral RNA generated from Pol I system is triphosphate or monophosphate. It can be speculated that viral RNA lacking modifications at the 5′ and 3′ ends is preferentially packaged and secreted into the culture supernatant.

Production of HCV RNA, proteins, and virions from cells transiently transfected with Pol I-driven plasmids. To examine HCV RNA replication and protein expression in cells transfected with pHHJFH1, pHHJFH1/GND, or virion production-defective mutants, pHHJFH1/ΔE and pHHJFH1/R783A/R785A, which possess an in-frame deletion of E1/E2 region and substitutions in the p7 region, respectively (19, 42, 49), RPA and Western blotting were performed 5 days p.t. (Fig. 2A, B, and D). Positive-strand HCV RNA sequences were more abundant than negative-strand RNA sequences in these cells. Positive-strand RNA, but not negative-strand RNA, was detected in cells transfected with the replication-defective mutant pHHJFH1/GND (Fig. 2A and B). Northern blotting showed that genome-length RNA was generated in pHHJFH1-transfected cells but not in pHHJFH1/GND-transfected cells (Fig. 2C).

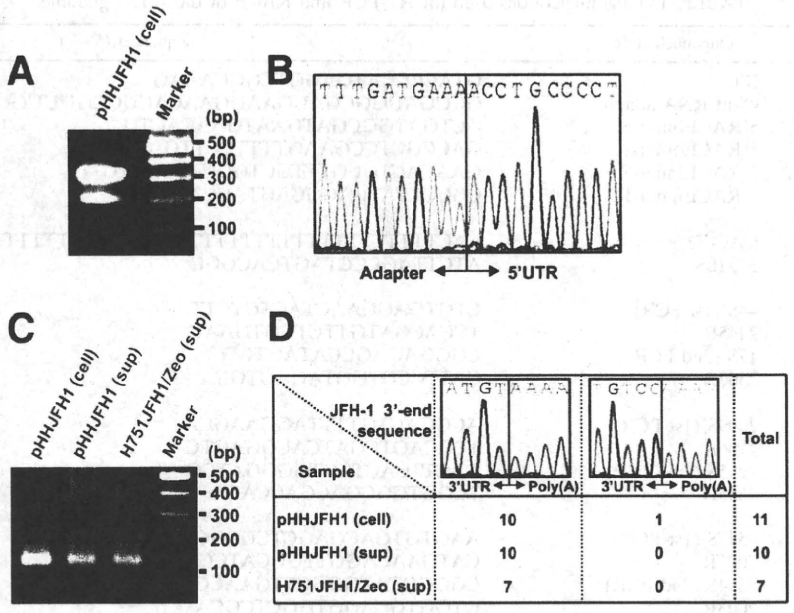

FIG. 1. Determination of the nucleotide sequences at the 5′-and 3′ ends of HCV RNA produced by the Pol I system. (A and B) 5′RACE and sequence analysis. A synthesized RNA adapter was ligated to RNA extracted from cells transfected with pHHJFH1. The positive-strand HCV RNA was reverse transcribed, and the resulting cDNA was amplified by nested PCR. The amplified 5′-end cDNA was separated by agarose gel electrophoresis (A), cloned, and sequenced (B). (C and D) 3′RACE and sequence analysis. RNA extracted from pHHJFH1-transfected cells, the culture supernatant of transfected cells, and the culture supernatant of H751JFH1/Zeo cells were polyadenylated, reverse transcribed, and amplified by PCR. The amplified 3′-end cDNA was separated by agarose gel electrophoresis (C), cloned, and sequenced (D).

As shown in Fig. 2D, the intracellular expression of core and NS5B proteins was comparable among cells transfected with pHHJFH1, pHHJFH1/ΔE, and pHHJFH1/R783A/R785A. Neither viral protein was detected in pHHJFH1/GND-transfected cells, suggesting that the level of viral RNA generated transiently from the DNA plasmid does not produce enough HCV proteins for detection and that ongoing amplification of the HCV RNA by the HCV NS5B polymerase allows a high enough level of viral RNA to produce detectable levels of HCV proteins.

To assess the release of HCV particles from cells transfected with Pol I-driven plasmids, core protein was quantified in culture supernatant by enzyme-linked immunosorbent assay (ELISA) or sucrose density gradient centrifugation. Core protein secreted from pHHJFH1-transfected cells was first detectable 2 days p.t., with levels increasing up to ~4 pmol/liter on day 6 (Fig. 3A). This core protein level was 4- to 6-fold higher than that in the culture supernatant of pHHJFH1/ΔE- or pHHJFH1/R783A/R785A-transfected cells, despite comparable intracellular core protein levels (Fig. 2D). Core protein was not secreted from cells transfected with pHHJFH1/GND (Fig. 3A). In another experiment, a plasmid expressing the secreted form of human placental alkaline phosphatase (SEAP) was cotransfected with each Pol I-driven plasmid. SEAP activity in culture supernatant was similar among all transfection groups, indicating comparable efficiencies of transfection (data not shown). Sucrose density gradient analysis of the concentrated supernatant of pHHJFH1-transfected cells indicated that the distribution of core protein levels peaked in the fraction of 1.17 g/ml density, while the peak of infectious titer was observed in the fraction of 1.12 g/ml density (Fig. 3B), which is consistent with the results of previous studies based on JFH-1-RNA transfection (23).

We next compared the kinetics of HCV particle secretion in the Pol I-driven system and RNA transfection system. Huh-7 cells, which have limited permissiveness for HCV infection (2), were transfected with either pHHJFH1 or JFH-1 RNA, and then cultured by passaging every 2 or 3 days. As shown in Fig. 3C, both methods of transfection demonstrated similar kinetics of core protein levels until 9 days p.t., after which levels gradually fell. However, significantly greater levels of core protein were detected in the culture of pHHJFH1-transfected cells compared to the RNA-transfected cells on day 12 and 15 p.t. This is likely due to an ongoing production of positive-strand viral RNA from transfected plasmids since RNA degradation generally occurs more quickly than that of circular DNA.

Establishment of stable cell lines constitutively producing HCV virion. To establish cell lines with constitutive HCV production, pHHJFH1/Zeo carrying HCV genomic cDNA and the Zeocin resistance gene were transfected into Huh7.5.1 cells. After approximately 3 weeks of culture with zeocin at a concentration of 0.4 mg/ml, cell colonies producing HCV core protein were screened by ELISA, and three clones were identified that constitutively produced the viral protein (H751JFH1/Zeo cells). Core protein levels within the culture supernatant of selected clones (H751-1, H751-6, and H751-50) were 2.0×10^4, 2.7×10^3, and 1.4×10^3 fmol/liter, respectively. Clone H751-1 was further analyzed. Indirect immunofluorescence with an anti-NS5A antibody showed fluorescent staining of NS5A in the cytoplasm of almost all H751JFH1/

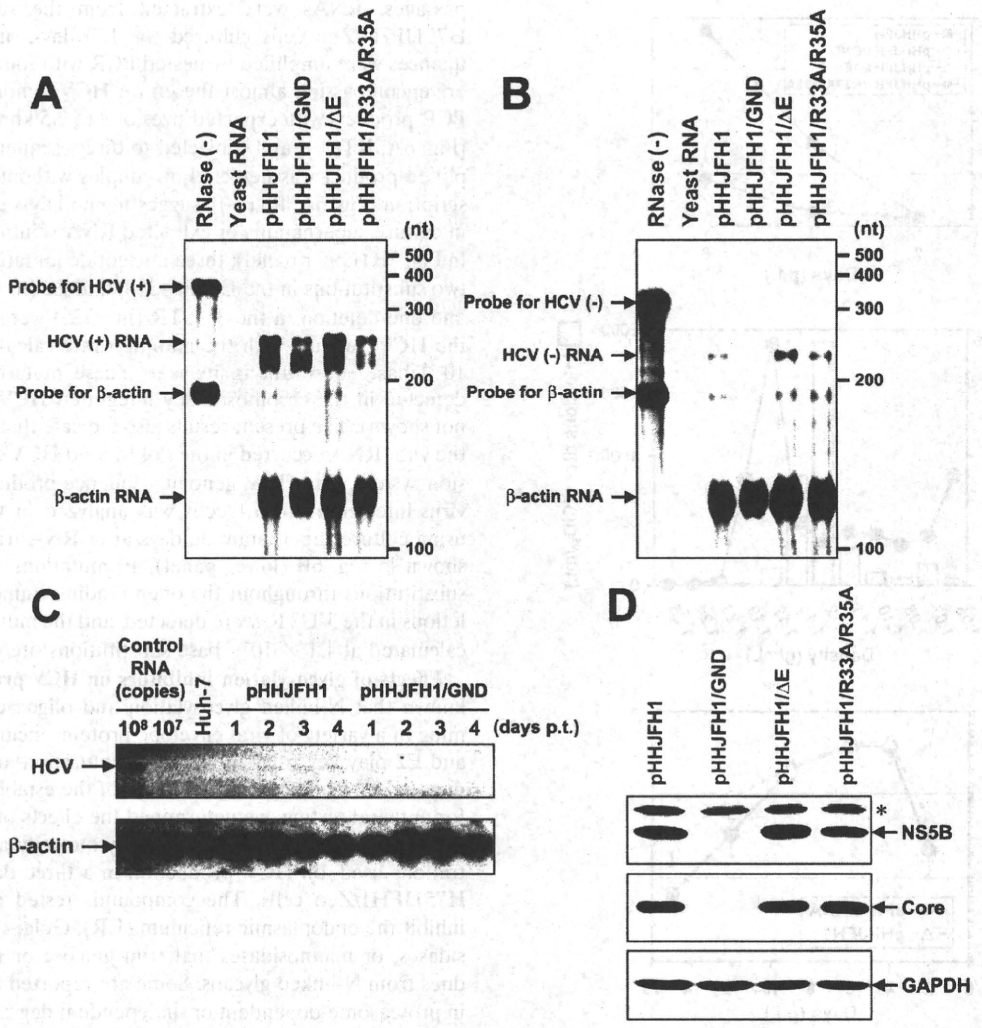

FIG. 2. HCV RNA replication and protein expression in cells transfected with Pol I-driven plasmids. (A and B) Assessment of HCV RNA replication by RPA. Pol I-driven HCV-expression plasmids were transfected into Huh-7 cells. Total RNA was extracted from the cells on day 5 p.t. and positive (A)- and negative (B)-strand HCV RNA levels were determined by RPA as described in Materials and Methods. In the RNase (−) lanes, yeast RNA mixed with RNA probes for HCV and human β-actin were loaded without RNase A/T1 treatment. In the yeast RNA lanes, yeast RNA mixed with RNA probes for HCV and human β-actin were loaded in the presence of RNase A/T1. (C) Northern blotting of total RNAs prepared from the transfected cells. Huh-7 cells transfected with pHHJFH1 or pHHJFH1/GND were harvested for RNA extraction through days 1 to 4 p.t. Control RNA, given numbers of synthetic HCV RNA; Huh-7, RNA extracted from naive cells. Arrows indicate full-length HCV RNA and β-actin RNA. (D) HCV protein expression in the transfected cells. Pol I-driven HCV-expression plasmids were transfected into Huh-7 cells, harvested, and lysed on day 6 p.t. The expression of NS5B, core, and GAPDH was analyzed by Western blotting as described in Materials and Methods. The asterisk indicates nonspecific bands.

Zeo cells (Fig. 4A), whereas no signal was detected in parental Huh7.5.1 cells (Fig. 4B). To determine where HCV RNA replicates in H751JFH1/Zeo cells, labeling of *de novo*-synthesized HCV RNA was performed. After interfering with mRNA production by exposure to actinomycin D, BrUTP-incorporated *de novo*-synthesized HCV RNA was detected in the cytoplasm of H751JFH1/Zeo cells (Fig. 4D) colocalized with NS5A in the perinuclear area (Fig. 4E and F).

Low mutation frequency of the viral genome in a long-term culture of H751JFH1/Zeo cells. The production level of infectious HCV from H751JFH1/Zeo cells at a concentration of $\sim 10^3$ $TCID_{50}$/ml was maintained over 1 year of culture (data not shown). It has been shown that both virus and host cells may adapt during persistent HCV infection in cell cultures, such that cells become resistant to infection due to reduced expression of the viral coreceptor CD81 (54). As shown in Fig. 5, we analyzed the cell surface expression of CD81 on the established cell lines by flow cytometry and observed markedly reduced expression on H751JFH1/Zeo cells compared to parental Huh7.5.1 cells. It is therefore possible that only a small proportion of HCV particles generated from H751JFH1/Zeo cells enter and propagate within the cells. The H751JFH1/Zeo system is thought to result in virtually a single cycle of HCV production from the chromosomally integrated gene and thus

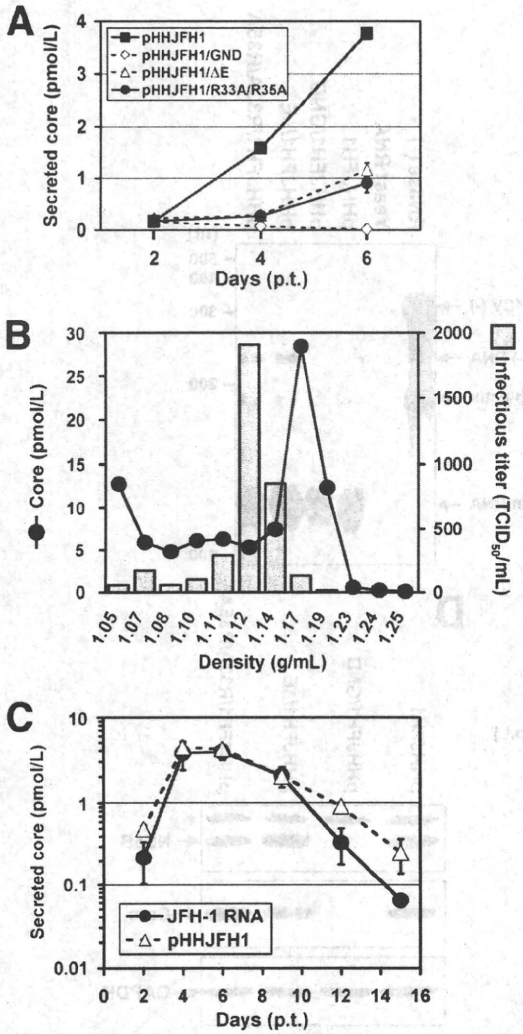

FIG. 3. HCV released from cells transfected with Pol I-driven plasmids. (A) HCV particle secretion from the transfected cells. The culture supernatant of Huh-7 cells transfected with Pol I-driven plasmids containing wild-type or mutated HCV genome were harvested on days 2, 4, and 6 and assayed for HCV core protein levels. The data for each experiment are averages of triplicate values with error bars showing standard deviations. (B) Sucrose density gradient analysis of the culture supernatant of pHHJFH1-transfected cells. Culture supernatant collected on day 5 p.t. was cleared by low-speed centrifugation, passed through a 0.45-μm-pore-size filter, and concentrated ~30-fold by ultrafiltration. After fractionating by sucrose density gradient centrifugation, the core protein level and viral infectious titer of each fraction were measured. (C) Kinetics of core protein secretion from cells transfected with pHHJFH1 or with JFH-1 genomic RNA. A total of 10^6 Huh-7 cells were transfected with 3 μg of pHHJFH1 or the same amount of *in vitro*-transcribed JFH-1 RNA by electroporation. The cells were passaged every 2 to 3 days before reaching confluence. Culture supernatant collected on the indicated days was used for core protein measurement. The level of secreted core protein (pmol/liter) is expressed on a logarithmic scale. The data for each experiment are averages of triplicate values with error bars showing standard deviations.

may yield a virus population with low mutation frequencies. To further examine this, we compared HCV genome mutation rates following production from H751JFH1/Zeo cells compared to cells constitutively infected with HCV after serial passages. RNAs were extracted from the supernatant of H751JFH1/Zeo cells cultured for 120 days, and cDNA sequences were amplified by nested PCR with four sets of primers encompassing almost the entire HCV genome (Table 1). PCR products with expected sizes of 2 to 2.5 kb were obtained [Fig. 6A, RT(+)] and subjected to direct sequencing. No amplified product was detected in samples without reverse transcription [Fig. 6A, RT(−)], suggesting no DNA contamination in culture supernatants or extracted RNA solutions. As shown in Fig. 5B (upper panel), three nucleotide mutations, including two substitutions in the E1 (nt 1218) and E2 (nt 1581) regions, and one deletion in the 3′ UTR (nt 9525) were found within the HCV genome with the mutation rate calculated at 9.6×10^{-4} base substitutions/site/year. These mutations were not detected in the chromosomally integrated HCV cDNA (data not shown). The present results also indicate that no splicing of the viral RNA occurred in the Pol I-based HCV JFH-1 expression system. The HCV genome sequence produced by JFH-1 virus-infected Huh7.5.1 cells was analyzed in the same way using culture supernatant 36 days after RNA transfection. As shown in Fig. 6B (lower panel), 10 mutations, including five substitutions throughout the open reading frame and five deletions in the 3′UTR, were detected, and the mutation rate was calculated at 1.1×10^{-2} base substitutions/site/year.

Effects of glycosylation inhibitors on HCV production. It is known that N-linked glycosylation and oligosaccharide trimming of a variety of viral envelope proteins including HCV E1 and E2 play key roles in the viral maturation and virion production. To evaluate the usefulness of the established cell line for antiviral testing, we determined the effects of glycosylation inhibitors, which have little to no cytotoxicity at the concentrations used, on HCV production in a three day assay using H751JFH1/Zeo cells. The compounds tested are known to inhibit the endoplasmic reticulum (ER), Golgi-resident glucosidases, or mannosidases that trim glucose or mannose residues from N-linked glycans. Some are reported to be involved in proteasome-dependent or -independent degradation of misfolded or unassembled glycoproteins to maintain protein integrity (4, 8, 27, 35).

As shown in Fig. 7A and B, treatment of H751JFH1/Zeo cells with increasing concentrations of *N*N-DNJ, which is an inhibitor of ER α-glucosidases, resulted in a dose-dependent reduction in secreted core protein. *N*N-DNJ was observed to have an IC_{50} (i.e., the concentration inhibiting 50% of core protein secretion) of ~20 μM. In contrast, KIF, which is an ER α-mannosidase inhibitor, resulted in a 1.5- to 2-fold increase in secreted core protein compared to control levels. The other five compounds did not significantly change core protein levels. We further determined the effects of *N*N-DNJ and KIF on the production of infectious HCV (Fig. 7C). As expected, *N*N-DNJ reduced the production of infectious virus in a dose-dependent manner, while production increased in the presence of KIF at 10 to 100 μM. Since *N*N-DNJ and KIF did not significantly influence viral RNA replication, as determined using the subgenomic replicon (data not shown), the present results suggest that some step(s), such as virion assembly, intracellular trafficking, and secretion, may be up- or downregulated depending on glycan modifications of HCV envelope proteins within the ER. Inhibitory effect of *N*N-DNJ was reproducibly observed using the cell line after 1 year of culturing

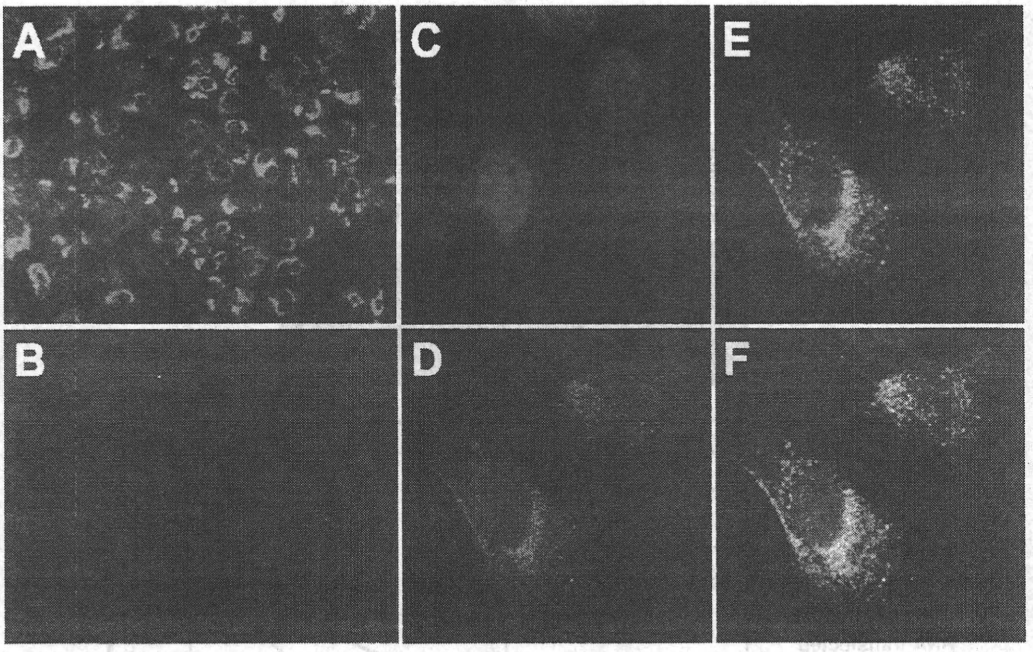

FIG. 4. Indirect immunofluorescence analysis of H751JFH1/Zeo cells. (A and B) H751JFH1/Zeo cells (A) and parental Huh7.5.1 cells (B) were immunostained with an anti-NS5A antibody. (C to F) The subcellular colocalization of *de novo*-synthesized HCV RNA and NS5A in H751JFH1/Zeo cells was analyzed. The cells were stained with DAPI (C), an anti-bromodeoxyuridine antibody (D), and an anti-NS5A antibody (E). The merge panel is shown in panel F.

(Fig. 7D). Under the same condition, the core protein secretion was inhibited by 28 and 58% with 10 and 100 nM BILN 2061, an NS3 protease inhibitor, respectively (Fig. 7D).

Replicon *trans*-packaging system. Recently, ourselves and others have developed a packaging system for HCV subgenomic replicon RNA sequences by providing *trans* viral core-NS2 proteins (1, 17, 41). Since viral structural proteins are not encoded by the subgenomic replicon, progeny virus cannot be produced after transfection. Thus, the single-round infectious HCV-like particle (HCV-LP) generated by this system potentially improves the safety of viral transduction. Here, in order to make the *trans*-packaging system easier to manipulate, we used a Pol I-driven plasmid to develop a transient two-plasmid expression system for the production of HCV-LP. pHH/SGR-Luc, which carries a bicistronic subgenomic reporter replicon with a Pol I promoter/terminator, or its replication-defective mutant, were cotransfected with or without a core-NS2 expression plasmid (Fig. 8A). The culture supernatant was then collected between days 2 and 5 p.t. and used to inoculate naive Huh7.5.1 cells. Reporter luciferase activity, as a quantitative measure of infectious virus production, was assessed in the cells 3 days postinoculation. As shown in Fig. 8B, reporter replication activity was easily detectable in cells inoculated with culture supernatant from cells cotransfected with pHH/

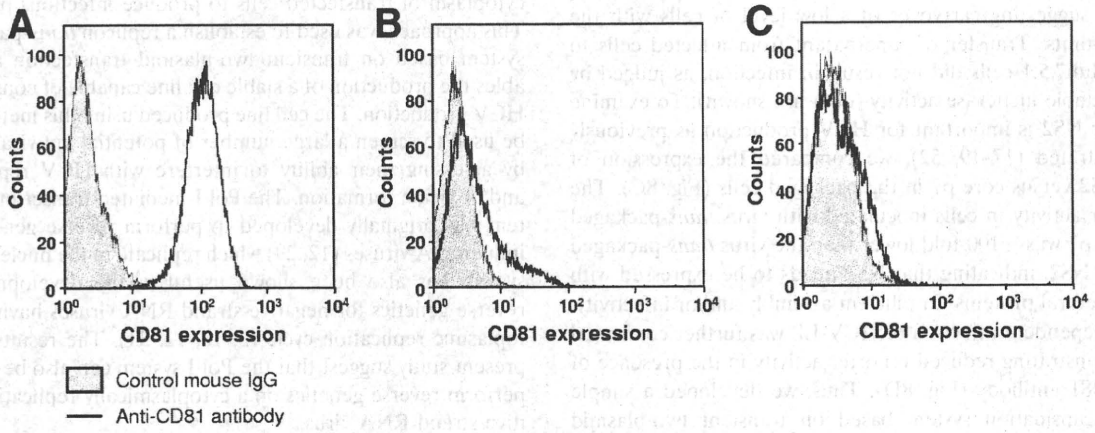

FIG. 5. Loss of CD81 expression in H751JFH1/Zeo cells. The cell surface expression of CD81 on Huh7.5.1 cells (A), H751JFH1/Zeo clone H751-1 (B), and clone H751-50 (C) was analyzed by flow cytometry after being stained with anti-CD81 antibody.